

1 **Sensitivity of the air-sea CO<sub>2</sub> exchange in the Baltic Sea and**  
2 **Danish inner waters to atmospheric short term variability**

3 **A. S. Lansø<sup>1</sup>, J. Bendtsen<sup>2</sup>, J. H. Christensen<sup>1,3</sup>, L. L. Sørensen<sup>1,3</sup>, H. Chen<sup>4,5</sup>, H. A. J.**  
4 **Meijer<sup>4</sup> and C. Geels<sup>1</sup>**

5 [1]{Department of Environmental Science, Aarhus University, 4000 Roskilde, Denmark}

6 [2]{Climate Lab, Symbion Science Park, Fruebjergvej 3, 2100 Copenhagen, Denmark}

7 [3]{Arctic Research Centre (ARC), Aarhus University, 8000C Aarhus, Denmark}

8 [4]{Centre for Isotope Research (CIO), Energy and Sustainability Research Institute Groningen (ESRIG),  
9 University of Groningen, Groningen, the Netherlands}

10 [5]{Cooperative Institute for Research in Environmental Sciences (CIRES), University of  
11 Colorado, Boulder, CO, USA}

12 Correspondence to: A. S. Lansø ([asla@envs.au.dk](mailto:asla@envs.au.dk))

13 **Abstract**

14 Minimising the uncertainties in estimates of air-sea CO<sub>2</sub> exchange is an important step toward  
15 increasing the confidence in assessments of the CO<sub>2</sub> cycle. Using an atmospheric transport model  
16 makes it possible to investigate the direct impact of atmospheric parameters on the air-sea CO<sub>2</sub> flux  
17 along with its sensitivity to e.g. short-term temporal variability in wind speed, atmospheric mixing  
18 height and the atmospheric CO<sub>2</sub> concentration. With this study the importance of high  
19 spatiotemporal resolution of atmospheric parameters for the air-sea CO<sub>2</sub> flux is assessed for six sub-  
20 basins within the Baltic Sea and Danish inner waters. A new climatology of surface water partial  
21 pressure of CO<sub>2</sub> ( $p\text{CO}_2^w$ ) has been developed for this coastal area based on available data from  
22 monitoring stations and underway  $p\text{CO}_2^w$  measuring systems. Parameterisations depending on wind  
23 speed were applied for the transfer velocity to calculate the air-sea CO<sub>2</sub> flux. Two model  
24 simulations were conducted – one including short term variability in atmospheric CO<sub>2</sub> (VAT), and  
25 one where it was not included (CAT).

26 A seasonal cycle in the air-sea CO<sub>2</sub> flux was found for both simulations for all sub-basins with  
27 uptake of CO<sub>2</sub> in summer and release of CO<sub>2</sub> to the atmosphere in winter. During the simulated

1 period 2005-2010 the average annual net uptake of atmospheric CO<sub>2</sub> for the Baltic Sea, Danish  
2 Straits and Kattegat was 287 Gg C yr<sup>-1</sup> and 471 Gg C yr<sup>-1</sup> for the VAT and CAT simulations,  
3 respectively. The obtained difference of 184 Gg C yr<sup>-1</sup> was found to be significant, and thus  
4 ignoring short term variability in atmospheric CO<sub>2</sub> does have a sizeable effect on the air-sea CO<sub>2</sub>  
5 exchange. The combination of the atmospheric model and the new pCO<sub>2</sub><sup>w</sup> fields has also made it  
6 possible to make an estimate of the marine part of the Danish CO<sub>2</sub> budget for the first time. A net  
7 annual uptake of 2613 Gg C yr<sup>-1</sup> was found for the Danish waters.

8 A large uncertainty is connected to the air-sea CO<sub>2</sub> flux in particular caused by the transfer velocity  
9 parameterisation and the applied pCO<sub>2</sub><sup>w</sup> climatology. However, as a significant difference of 184 Gg  
10 C yr<sup>-1</sup> is obtained between the VAT and CAT simulations, the present study underlines the  
11 importance of including short term variability in the atmospheric CO<sub>2</sub> concentration in future model  
12 studies of the air-sea exchange in order to minimise the uncertainty.

## 13 **1 Introduction**

14 The capacity of ocean and land to take up and re-emit atmospheric CO<sub>2</sub> has a dominating effect on  
15 the greenhouse gas balance, and hence changes in climate. Currently, the land areas and the global  
16 oceans are estimated to take up about 27% and 28 %, respectively, of the CO<sub>2</sub> emitted by  
17 anthropogenic sources (Le Quéré et al., 2013).

18 In recent years the biogeochemically active coastal seas have been given increased attention  
19 (Borges et al., 2006; Chen et al., 2013; Mørk et al., 2014). Although such coastal waters only  
20 amount to 7% of the global oceans, high inputs, production, degradation and export of organic  
21 matter might result in coastal air-sea CO<sub>2</sub> fluxes contributing a great deal more than 7% to the  
22 global air-sea flux (Gattuso et al., 1998). Due to the high heterogeneity of these areas, coastal CO<sub>2</sub>  
23 fluxes are prone to large uncertainties. Several studies agree that continental shelves, in general, act  
24 as sinks, while estuaries act as sources of CO<sub>2</sub> to the atmosphere. However, global estimates vary in  
25 size according to applied methodology, with oceanic uptake in shelf areas between 0.21 Pg C yr<sup>-1</sup>  
26 and 0.40 Pg C yr<sup>-1</sup>, and release from estuaries in the range of 0.10 Pg C yr<sup>-1</sup> to 0.50 Pg C yr<sup>-1</sup> (Cai,  
27 2011; Chen et al., 2013; Chen and Borges, 2009; Laruelle et al., 2010). The poor coverage of  
28 observations in both space and time makes validation of these global estimates difficult.

29 In order to better quantify the impact of coastal regions on the global carbon budget, detailed  
30 studies of the processes at the regional scale are necessary (Kulinski and Pempkowiak, 2011). A

1 coastal region that has been well studied is the Baltic Sea. The Baltic Sea is a high latitude inner  
2 shelf sea connected to the North Sea through the shallow transition zone of the Danish Straits, and  
3 enclosed by land with various terrestrial ecosystems and densely populated areas. Seasonal  
4 amplitudes of up to 400  $\mu\text{atm}$  are observed in the partial pressure of  $\text{CO}_2$  ( $p\text{CO}_2^w$ ) in the Baltic Sea  
5 (Thomas and Schneider, 1999) with maximum values of  $p\text{CO}_2^w$  found in winter and minimum  
6 during summer. Since the difference between the  $p\text{CO}_2$  level in the ocean and the atmosphere  
7 controls the direction of the air-sea  $\text{CO}_2$  flux, this is an indication of the pronounced seasonal  
8 variation of the flux in the Baltic Sea, with outgassing of  $\text{CO}_2$  to the atmosphere during winter and  
9 uptake during summer (Thomas et al., 2004; Thomas and Schneider, 1999). Despite numerous  
10 studies, it is still uncertain, whether the Baltic Sea currently acts as a net sink or source of  
11 atmospheric  $\text{CO}_2$ , as previous studies have given ambiguous results varying from  $-4.3$  to  $2.7 \text{ g C m}^{-2}$   
12  $\text{yr}^{-1}$  for the entire Baltic Sea region (Gustafsson et al., 2014; Kulinski and Pempkowiak, 2011;  
13 Norman et al., 2013). Thereby, it is also difficult to project how the Baltic Sea will contribute to the  
14 global carbon budget in the future. Moreover, the region may possibly have changed from being a  
15 net source to a net sink of atmospheric  $\text{CO}_2$ , due to the industrialization and the enormous input of  
16 nutrients (Omstedt et al., 2009). These inputs will, however, likely change in the future due to  
17 changes in climate and anthropogenic activities (Geels et al., 2012; Langner et al., 2009).

18 As the Baltic Sea is bordered by land areas, the atmospheric  $\text{CO}_2$  concentration found here will be  
19 directly affected by continental air leading to a greater temporal and spatial variability in the  $\text{CO}_2$   
20 level, than what is found over open oceans. The impact of temporal variations in atmospheric  $\text{CO}_2$   
21 on the air-sea  $\text{CO}_2$  exchange has been discussed by Rutgersson et al. (2008) and (2009). They show  
22 an overestimation in the amplitude of the seasonal cycle for calculated air-sea  $\text{CO}_2$  fluxes, when  
23 using a constant annual mean value of atmospheric  $\text{CO}_2$  concentration instead of daily levels of the  
24 atmospheric concentration. Annually, the difference was less than 10 % between the two cases, but  
25 weekly flux deviations of 20 % were obtained. This indicates how synoptic variability in the  
26 atmosphere cannot always be ignored (Rutgersson et al., 2009). Further, Rutgersson et al. (2008)  
27 note that the uncertainties connected with the transfer velocity are much greater than uncertainties  
28 related to temporal variations in atmospheric  $\text{CO}_2$ . However, it is still worthwhile to minimise the  
29 bias in the estimation of the flux by including detailed information of the atmospheric  $\text{CO}_2$   
30 concentration. The short term variability (hourly) of both meteorology and atmospheric  $\text{CO}_2$   
31 concentrations is not always accounted for or has not been discussed in previous estimates of the

1 air-sea CO<sub>2</sub> fluxes in the Baltic Sea (Algesten et al., 2006; Gustafsson et al., 2014; Kulinski and  
2 Pempkowiak, 2011; Löffler et al., 2012; Norman et al., 2013; Wesslander et al., 2010) .

3 The present study aims to determine the importance of the short-term variability in atmospheric  
4 CO<sub>2</sub> concentrations on the net air-sea CO<sub>2</sub> flux of the Baltic Sea and Danish inner waters (which  
5 consists of Kattegat and the Danish straits; Øresund and the Belt Seas). A modelling approach is  
6 applied, which includes both short-term (hourly to synoptic) and long-term (seasonal to inter-  
7 annual) variability in the atmospheric CO<sub>2</sub> concentrations. The analysis is carried out by  
8 constructing a meso-scale model framework based on an atmospheric transport model covering the  
9 study region with high resolution in both space and time. The model includes a new spatial  $p\text{CO}_2^w$   
10 climatology developed especially for the investigated marine area, as existing climatologies do not  
11 cover this area. The advantages of the present study are that the same and consistent method is  
12 applied to the entire Baltic Sea and Danish inner waters, and that the impact of spatial and temporal  
13 short term variability in atmospheric parameters will be investigated in more detail than in the  
14 previous studies of this region.

15 Recently, national CO<sub>2</sub> budgets that include both anthropogenic and natural components have been  
16 estimated for various countries (Meesters et al., 2012; Smallman et al., 2014). The present study is  
17 likewise part of a national project: Ecosystem Surface Exchange of Greenhouse Gases in an  
18 Environment of Changing Anthropogenic and Climate forcing (ECOCLIM) that is to determine the  
19 CO<sub>2</sub> budget for Denmark. For that reason the present study will also estimate the marine component  
20 of the Danish CO<sub>2</sub> budget.

21 In Sect. 2 the study area, the applied surface fields of  $p\text{CO}_2^w$  and the model frame work are  
22 described. Results are presented in Sect. 3, leading to a discussion in Sect. 4, and concluding  
23 remarks in Sect. 5.

## 24 **2 Study setup**

### 25 **2.1 Study area**

26 The marine areas investigated in this study are shown in Fig. 1. In the following a short introduction  
27 to these heterogeneous marine areas is given, as well as a description of the overall atmospheric  
28 CO<sub>2</sub> field in the region.

1 The Baltic Sea is a semi-enclosed continental shelf sea area with a large volume of river runoff  
2 adding a substantial amount of nutrients and terrestrial carbon to the Baltic Sea (Kulinski and  
3 Pempkowiak, 2011). The circulation in the Baltic Sea is influenced by a relatively large runoff from  
4 the surrounding drainage areas, and this causes a low-salinity outflowing surface water mass from  
5 the area. The Baltic Sea can, therefore, be considered as a large estuary. Inflow of high-salinity  
6 water from the North Sea ventilates the bottom waters of the Baltic Sea, and the exchange between  
7 these water masses occurs through the shallow North Sea/Baltic Sea transition zone centred around  
8 the Danish Straits (Bendtsen et al., 2009). Ice coverage is observed in the northern part of Baltic Sea  
9 during winter (Löffler et al., 2012), which has implications for the air-sea exchange of CO<sub>2</sub>. The ice  
10 extent in the Baltic Sea during 2005-2010 fluctuated between average conditions in the winter  
11 2005-2006 (ice cover of 210.000 km<sup>2</sup>), a general mild period in the winters between 2007-2009  
12 (with a minimum ice cover of 49.000 km<sup>2</sup> in 2007-2008) and a severe winter condition in 2010-  
13 2011 where the sea ice extent reached a maximum value of 309.000 km<sup>2</sup> (Vainio et al., 2011). Thus,  
14 there was no apparent trend of the sea ice extent in the simulation period.

15 Atmospheric concentrations of CO<sub>2</sub> in the Baltic region have a greater seasonal amplitude than at  
16 e.g. Mauna Loa, Hawaii, which often is referred to as a global reference for the atmospheric CO<sub>2</sub>  
17 background, due to the remoteness of the site. The larger seasonal amplitude over the Baltic can be  
18 explained by the difference in latitude between the studied area (54-66°N) and Mauna Loa (20°N),  
19 and the undisturbed air at the high altitude site of Mauna Loa compared to the semi-enclosed Baltic  
20 Sea (Rutgersson et al., 2009). The study by Rutgersson and colleagues also showed that the  
21 atmospheric CO<sub>2</sub> concentration in the southern part of the Baltic Sea is more affected by regional  
22 anthropogenic and terrestrial sources and sinks, than the more remote northern part of the Baltic Sea  
23 area.

## 24 **2.2 Surface water pCO<sub>2</sub><sup>w</sup> climatology**

25 Model calculations of the surface air-sea gas exchange of CO<sub>2</sub> are parameterised in terms of the  
26 difference in partial pressure of CO<sub>2</sub> (i.e.  $\Delta p\text{CO}_2$ ) between the atmosphere and the ocean surface.  
27 The global climatology of oceanic surface pCO<sub>2</sub><sup>w</sup> by Takahashi et al. (2009) is commonly used in  
28 atmospheric transport models of CO<sub>2</sub> (e.g. Geels et al., 2007; Sarrat et al., 2009), and is also applied  
29 here for areas outside the Baltic Sea and the Danish inner waters. However, this climatology does  
30 not cover the Baltic Sea area, and therefore, a new Baltic Sea climatology has been created and

1 merged with the climatology of Takahashi et al. (2009) in the model domain towards the North Sea  
2 and the Northern North Atlantic.

3 Available  $p\text{CO}_2^w$  surface measurements and water chemistry data from the Baltic Sea and the  
4 Danish inner waters are combined in six sub-domains of the Baltic Sea to provide monthly averaged  
5  $p\text{CO}_2^w$  values for this new climatology. The sub-domains cover Skagerrak, Kattegat and the Belt Sea  
6 (henceforth referred to just as Kattegat), the Western Baltic Sea, the Baltic Proper, the Gulf of  
7 Finland, the Bothnian Sea and the Bay of Bothnia. Two data sets are analysed; one from marine  
8 stations (stationary) and the other obtained from ships (underway). All available data collected since  
9 year 2000 is included in the analysis (Fig. 1). Hence, measurements from a depth of 5 m from all  
10 stations were averaged for the period 2000-12, and underway  $p\text{CO}_2^w$  measurements from the surface  
11 layer (surface intake approximately 5m) were averaged for the period 2000-11. From the two data  
12 sets monthly mean values for each sub-domain are determined.

13 Surface measurements of salinity, temperature, alkalinity and pH from six marine measuring  
14 stations (operated by the Swedish Meteorological and Hydrological Institute, SMHI (Shark Data  
15 Base, 2013)) are applied to calculate the surface  $p\text{CO}_2^w$  values by a similar approach as described in  
16 Wesslander et al. (2010). The six stations are located from the central Skagerrak to the Bay of  
17 Bothnia (Fig. 1), but no measurements are available from the Gulf of Finland. A relatively high  
18 frequency of observations is obtained at the six monitoring stations with the number of observations  
19 in each month ranging between 4-8 at station A17, 15-36 at station Anholt E, 6-18 at station BY5,  
20 7-17 at station BY15, 1-5 at station C3 (but no data representing November) and 2-10 at station F9  
21 (but no data representing January, February and November).

22 Surface levels of  $p\text{CO}_2^w$  from the central Baltic Sea (Schneider and Sadkowiak, 2012) have been  
23 measured by underway-  $p\text{CO}_2^w$  systems (Körtzinger et al., 1996; Schneider et al., 2006) from cargo  
24 and research ships. In particular, a route between Germany (Kiel) and Finland (Helsinki) has  
25 regularly been monitored from cargo-ships, whereas no measurements are available in the northern  
26 part of the Baltic Sea, the Danish straits, Kattegat and Skagerrak. Good data coverage of underway  
27  $p\text{CO}_2^w$  measurements is obtained in the sub-domain of the Western Baltic Sea, with the number of  
28 observations in each month ranging between 9.000 and 55.000, and in the Baltic Proper, where the  
29 corresponding number of observations ranges from 20.000 to 116.000. In the Bothnian Sea the  
30 number of observations ranges from 2.000 to 77.000, but there are no observations in December.

1 Only a single month (March) is represented in the Bay of Bothnia with about 5000 observations.  
2 The Gulf of Finland is represented with observations ranging from 3000 and 18.000 each month.  
3 The stationary data from the monitoring stations and the underway data have been combined in  
4 such a manner that if underway data exists for a sub-domain, these data is used for the  $p\text{CO}_2^w$  fields  
5 in the given subdomain. Otherwise, measurements from the monitoring stations are used to  
6 calculate the  $p\text{CO}_2^w$  fields. Thus,  $p\text{CO}_2^w$  fields for Skagerrak, Kattegat, and the Bay of Bothnia are  
7 calculated solely based on data from the SMHI stations. The  $p\text{CO}_2^w$  fields for the Western Baltic  
8 Sea, the Baltic Proper, the Gulf of Finland and the Bothnian Sea are obtained from the underway  
9 measurements of  $p\text{CO}_2^w$ , except for December in the Bothnian Sea, which is represented by the  
10 monitoring station C3. The data used to obtain the monthly averages of surface  $p\text{CO}_2^w$  in each sub-  
11 domain have all been normalised to year 2000 using an annual increase in  $\text{CO}_2$  of  $1.9 \mu\text{atm yr}^{-1}$   
12 found for the central Baltic Sea (Wesslander et al., 2010).

13 The resulting  $p\text{CO}_2^w$  climatology for the Baltic Sea and Danish inner waters is combined with the  
14 global open ocean  $p\text{CO}_2^w$  climatology from Takahashi et al. (2009). This climatology is calculated  
15 for a global oceanic grid with a horizontal resolution of  $5^\circ \times 4^\circ$  in longitude and latitude,  
16 respectively. Consequently, this field has an even coarser spatial resolution than the sub-domains  
17 defined in the Baltic Sea area. The global climatology is by Takahashi and co-workers referenced to  
18 the year 2000 with an annual trend of  $1.5 \mu\text{atm yr}^{-1}$ . This trend is also used to extrapolate the global  
19 data for year 2000 to the proceeding years covered in this study. Note that the trend used for the  
20 Baltic Sea and Danish inner waters is  $1.9 \mu\text{atm yr}^{-1}$ , as this trend is shown to match this particular  
21 area. However, the difference in annual trends between the two climatologies is so small compared  
22 to the absolute  $p\text{CO}_2^w$  values, thus it is reasonable to assume that the impact on the current results  
23 will be insignificant.

24 The monthly averaged  $p\text{CO}_2^w$  values show a characteristic seasonal pattern at all monitoring stations  
25 and for the underway  $p\text{CO}_2^w$  data (Fig. 2, Table S1 and Fig. S1 in the Supp. Material). The surface  
26  $p\text{CO}_2^w$  is under-saturated during spring and summer and super-saturated during fall and winter (Fig.  
27 3a). However, there is a large spatial gradient in the seasonal amplitude from Skagerrak and into the  
28 Baltic Sea. A seasonal amplitude of about  $140 \mu\text{atm}$  characterises the variation in Skagerrak and  
29 Kattegat, where the  $p\text{CO}_2^w$  varies between  $275 \mu\text{atm}$  and  $420 \mu\text{atm}$ , and the surface water is only  
30 slightly super-saturated during the winter months. In the Baltic Sea a relatively large seasonal  
31 amplitude of up to  $400 \mu\text{atm}$  is observed, as primary production during the growing season, i.e.

1 spring and summer, causes a large uptake of total dissolved inorganic carbon in the surface layer  
2 and contributes to lowering the surface  $p\text{CO}_2^{\text{W}}$  values. The data shows how biological uptake causes  
3 a reduction of surface  $p\text{CO}_2^{\text{W}}$ , despite the general warming during the summer months, which  
4 normally tends to increase the  $p\text{CO}_2^{\text{W}}$  in the surface water. During fall and winter, the surface  
5  $p\text{CO}_2^{\text{W}}$  values increase because sub-surface waters enriched in total dissolved inorganic carbon from  
6 remineralisation of organic matter during the summer are mixed into the surface layer. In the areas  
7 north-east of the Western Baltic Sea in particular, this allows for high monthly averaged surface  
8  $p\text{CO}_2^{\text{W}}$  values of 460 - 530  $\mu\text{atm}$  during winter with the largest average winter values observed in the  
9 Gulf of Finland.

10 The calculated  $p\text{CO}_2^{\text{W}}$  values at the monitoring stations agree well the underway  $p\text{CO}_2^{\text{W}}$  data. The  
11 underway  $p\text{CO}_2^{\text{W}}$  data includes both temporal and spatial variability within each sub-domain during  
12 the period since 2000. Therefore, their standard deviations (SD) are larger than the SDs from the  
13 monitoring stations, which mainly arise due to inter-annual variability in the period. Two sub-  
14 domains, the Western Baltic Sea and the Baltic Proper, have good data coverage from both the  
15 monitoring stations and underway  $p\text{CO}_2^{\text{W}}$  data. The stations, BY5 and BY15, that represent the  
16 Western Baltic Sea and the Baltic Proper, respectively, have lower surface  $p\text{CO}_2^{\text{W}}$  values during the  
17 summer period than the underway  $p\text{CO}_2^{\text{W}}$  data, but the difference between the two data sets are  
18 within their SD.

### 19 **2.3 Model framework**

20 The model framework is based upon the Danish Eulerian Hemispheric Model (DEHM) - a well  
21 validated three dimensional large scale atmospheric chemical transport model (Brandt et al., 2012;  
22 Christensen, 1997). DEHM is based on the equation of continuity and uses terrain following sigma  
23 levels as vertical coordinates. Here, 29 vertical levels are distributed between the surface and 100  
24 hPa with a higher density of vertical levels in the lower part of the atmosphere. The main domain of  
25 DEHM covers the Northern Hemisphere with a horizontal grid resolution of 150 km x 150 km  
26 using a polar stereographic projection true at 60°N. Furthermore, DEHM has nesting capabilities  
27 allowing for a nest over Europe with a resolution of 50 km x 50 km, a nest of Northern Europe with  
28 an approximate resolution of 16.7 km x 16.7 km, and a 5.6 km x 5.6 km nest covering Denmark. In  
29 order to cover the Baltic Sea and the Danish marine areas in focus, a setup with two nests is applied  
30 in the current study (the European and the Northern European nests). The main domain and the



1 nests each comprise of 96 x 96 grid points. This study uses a modified version of DEHM solely  
2 simulating transport and exchange of CO<sub>2</sub> (Geels et al., 2002; Geels et al., 2004; Geels et al., 2007),  
3 but with an updated description of the surface exchange of CO<sub>2</sub> (described in Sect. 2.2.1). DEHM is  
4 driven by meteorological data from the meteorological model MM5v3.7 (Grell et al., 1995) using  
5 National Centers for Environmental Prediction, NCEP, data as input.

### 6 2.3.1 Model inputs

7 To accurately simulate the atmospheric content of CO<sub>2</sub>, a number of CO<sub>2</sub> sources and sinks within  
8 the model domain as well as inflow at the lateral boundaries are required together with a  
9 background concentration. The atmospheric concentration of CO<sub>2</sub> ( $X_{atm}$ ) can be described by

$$10 \quad X_{atm} = X_{ff} + X_{bio} + X_{fire} + X_{ocn} + X_{background} \quad (2.1)$$

11 where  $X_{ff}$  is the contribution of CO<sub>2</sub> from fossil fuel emissions,  $X_{fire}$  from vegetation fires, and  $X_{bio}$   
12 and  $X_{ocn}$  are the contribution to the atmospheric concentration from exchange of CO<sub>2</sub> with the  
13 terrestrial biosphere and ocean, respectively.  $X_{background}$  is the atmospheric background of CO<sub>2</sub>.

#### 14 *Fossil Fuel ( $X_{ff}$ )*

15 Fossil fuel emissions for the domain covering the Northern Hemisphere are implemented in DEHM  
16 from the Carbon Tracker (hereafter referred to as CT) simulation system (CarbonTracker  
17 CT2011\_oi, 2013; Peters et al., 2007). This emission map has a three hourly temporal resolution on  
18 a 1°x1° grid.

19 For the European area, the CT values are replaced by a fossil fuel emission inventory with a higher  
20 spatiotemporal resolution (hourly, 10 km x 10 km) developed by the Institute of Energy Economics  
21 and the Rational Use of Energy (Pregger et al., 2007).

22 For the area of Denmark, emissions with an even finer spatial resolution of 1 km x 1 km are applied  
23 obtained from the Department of Environmental Science, Aarhus University. These are based on  
24 the Danish national inventory submitted yearly to UNFCCC (United Nations Framework  
25 Convention on Climate Change) and constructed from energy statistics, point source and statistic  
26 sub-models (Plejdrup and Gyldenkærne, 2011).

27 As the European and Danish emission inventories are for the years 2005 and 2011, respectively,  
28 these inventories are scaled to total yearly national estimates of carbon emissions from fossil fuel

1 consumption conducted by the Carbon Dioxide Information Analysis Center, CDIAC, in order to  
2 account for the year to year change in emissions (Boden et al., 2013).

### 3 *Biosphere ( $X_{bio}$ )*

4 Terrestrial biosphere fluxes from the CT system, with a spatial resolution of  $1^\circ \times 1^\circ$  and a temporal  
5 resolution of three hours, are applied in DEHM. In the CT assimilation system the Carnegie-Ames  
6 Stanford Approach (CASA) biogeochemical model is used for prior fluxes (Giglio et al., 2006; van  
7 der Werf et al., 2006). The prior terrestrial biosphere fluxes are optimised in the CT assimilation  
8 system by atmospheric observations of  $\text{CO}_2$ . Via this atmospheric inversion a best guess of surface  
9 fluxes is obtained, and the optimised fluxes are implemented in DEHM.

### 10 *Fires ( $X_{fire}$ )*

11  $\text{CO}_2$  emissions due to vegetation fires are obtained from the CT fire module and applied in DEHM.  
12 The CT fire module is based on the Global Fire Emission Database, GFEDv3.1, and CASA, while  
13 the burned area from GFED is based on MODIS satellite observations of fire counts. The resolution  
14 is likewise three hourly on a  $1^\circ \times 1^\circ$  grid.

### 15 *Ocean ( $X_{ocn}$ )*

16 The  $\text{CO}_2$  flux ( $F$ ) at the air-sea interface is calculated using the relation:  $F = k\alpha\Delta p\text{CO}_2$ , where,  $k$  is  
17 the exchange coefficient,  $\alpha$  is the gas solubility and  $\Delta p\text{CO}_2$  is the difference in partial pressure of  
18  $\text{CO}_2$  between the surface water and the overlying air. The gas solubility of  $\text{CO}_2$  is determined from  
19 Weiss (1974) and depends on the water temperature and salinity. A  $0.25^\circ \times 0.25^\circ$  salinity map is  
20 implemented in DEHM for the calculation of  $\text{CO}_2$  solubility (Boyer et al., 2005). To calculate  
21  $\Delta p\text{CO}_2$  the surface  $p\text{CO}_2^w$  fields described in Sect. 2.2 are applied together with the concentration of  
22  $\text{CO}_2$  in the lowest atmospheric layer in DEHM.

23 No standardised parameterisation of the transfer velocity,  $k$ , exists, but  $k$  is most often  
24 parameterised as a power function of the wind speed (Garbe et al., 2014; Rutgersson et al., 2008)  
25 normalised to the Schmidt's number ( $Sc$ ) according to Wanninkhof, (1992). In the present study we  
26 use the parameterisation of Wanninkhof (1992) (hereafter referred to as W92). This  
27 parameterisation has been used in many previous studies within the study area (Löffler et al., 2012;  
28 Rutgersson et al., 2008; Wesslander et al., 2010), and by using W92 this allows for a direct  
29 comparison of the estimated fluxes. W92 is a function of the wind speed at 10 m above the surface  
30 ( $u_{10}$ ) and when normalised to  $Sc$  at  $20^\circ\text{C}$  in salt water it has the form:

$$k_{660} = (0.31u_{10}^2) \sqrt{\frac{660}{Sc}} \quad (2.2)$$

However, a few additional parameterisations that could be more representative for the study area are also tested. One is Nightingale et al. (2000), who estimate a transfer velocity based on tracer gas measurements in the North Sea of:

$$k_{660} = (0.333u_{10} + 0.222u_{10}^2) \sqrt{\frac{660}{Sc}} \quad (2.3)$$

Another is by Weiss et al. (2007), who have carried out measurements using eddy covariance techniques in the Arkona basin located within the Baltic Sea to estimate an accurate  $k$  for this particular area. This parameterisation takes the form:

$$k_{660} = (0.365u_{10}^2 + 0.46u_{10}) \sqrt{\frac{660}{Sc}} \quad (2.4)$$

The parameterisation by Weiss et al. (2007) often yields greater values than other transfer velocity parameterisations; however, it will be applied here, as the experiment was conducted within the study area.

Sea ice coverage is in DEHM obtained from NCEP. The sea ice coverage is implemented in the calculations of the air-sea CO<sub>2</sub> exchange, such that the flux in a grid cell is reduced by the fraction of sea ice. If the fraction of sea ice coverage is 1, the entire grid cell will be covered with ice, and no exchange of CO<sub>2</sub> will take place between the ocean and atmosphere. Recent studies have shown that CO<sub>2</sub> exchange between ice-covered sea and the atmosphere does take place, but to what extent has not yet been quantified (Parmentier et al., 2013; Sørensen et al., 2014). For that reason the exchange over sea ice is not accounted for here.

$k_{660}$ ,  $\alpha$  and  $\Delta p\text{CO}_2$  are calculated at each time step of the model simulation (The time step of the model varies between ca. 3-20 minutes depending of e.g. the nest). Consequently, the air-sea CO<sub>2</sub> flux has the same temporal resolution as the simulated atmospheric CO<sub>2</sub>.

### *Atmospheric Background ( $X_{background}$ )*

The level of atmospheric CO<sub>2</sub> has been increasing since pre-industrial times. It is not feasible to simulate this entire time period with the model system as to replicate this build-up. Therefore, an atmospheric background of CO<sub>2</sub> is needed. The atmospheric background of CO<sub>2</sub> is established on the basis of the NOAA ESRL GLOBALVIEW-CO2 data product using observations from the Baltic Station, BAL (lat=55°35' N, lon= 17°22' E)(GLOBALVIEW-CO2, 2013). BAL lies within the

1 area of interest, but far from local sources and sinks. It can, therefore, be assumed to represent the  
2 atmospheric background level in the study area. The atmospheric background of CO<sub>2</sub> is calculated  
3 based on the following equation:

$$4 \quad X_{background} = X_{CO_2_{2000}} + 1.91(year - 2000) + 0.16month \quad (2.5)$$

6 Here  $X_{CO_2_{2000}} = 370.15$  ppm is the mean CO<sub>2</sub> concentration at the station in 2000, *year* and  
7 *month* is the simulated year and month, and 1.91 and 0.16 represent the yearly and monthly trend of  
8 atmospheric CO<sub>2</sub>. The trends are based on the times series at BAL for the period 2000-2010, in  
9 order to get a representative overall trend for the period in focus here (2005-2010).

#### 10 *Boundary conditions*

11 DEHM only covers the Northern Hemisphere; hence boundary conditions for the main domain are  
12 needed at the lateral boundaries towards the Southern Hemisphere, as to account for inflow from the  
13 Southern Hemisphere. Three dimensional atmospheric mole fractions of CO<sub>2</sub> from the CT system  
14 are applied at these boundaries.

### 15 **3 Results**

#### 16 **3.1 Model evaluation**

17 The period 2005-2010 is simulated by DEHM with setup and fluxes as described in Sect. 2. The  
18 performance of the model for this period is evaluated by comparing simulated atmospheric CO<sub>2</sub>  
19 concentrations against observed. The comparison is made at six stations within the study area,  
20 where both remote continental (PAL), marine (F3, MHD, OST, WES) and anthropogenic (LUT)  
21 influenced stations are represented.

22 Measured and simulated atmospheric CO<sub>2</sub> from the marine site Östergarnsholm, Sweden (OST,  
23 57°27' N, 18°59' E) and the anthropogenic continental site Lutjewad, the Netherlands (LUT, 53°40'  
24 N, 6°31' E)(van der Laan et al., 2009) are shown for year 2007 in Fig. 4. The Östergarnsholm  
25 marine micrometeorological field station has been running semi-continuously since 1995,  
26 measuring atmospheric CO<sub>2</sub> since 2005. The site has been shown to represent marine conditions  
27 and is describe further in Rutgersson et al. (2008) and Högström et al. (2008). Hourly mean  
28 concentrations are plotted for simulated and measured atmospheric CO<sub>2</sub>, and at both sites a large  
29 diurnal variability is seen in the observations. The model is not able to capture the large amplitude

1 in the diurnal cycle, but correlations of 0.75 and 0.71 are obtained for LUT and OST, respectively.  
2 The root mean square errors, RMSE, are 9.6 ppm and 8.8 ppm, respectively. These high RMSEs are  
3 linked to the underestimation of the diurnal cycle in the model. Earlier model studies have shown  
4 the same tendency to underestimate the observed variability (e.g. Geels et al., 2007). The  
5 underestimation of the diurnal cycle by DEHM is most likely caused by the coarse spatial resolution  
6 of the biosphere fluxes. Further, weekly averages are made for both observed and modelled  
7 concentrations of atmospheric CO<sub>2</sub> (see Fig. 4). Improvements are obtained in both correlation and  
8 RMSE to 0.89 and 5.3 ppm for LUT, and 0.91 and 5.6 ppm for OST. Synoptic scale variability is  
9 seen in the atmospheric CO<sub>2</sub> concentration in both the simulated and observed time-series.  
10 Especially at LUT large positive spikes are seen due to the influence of air from densely populated  
11 and industrialised regions.

12 Flask measurements of CO<sub>2</sub> at F3, an oil and gas platform in the Dutch Exclusive Economic Zone  
13 of the North Sea approximately 200 km north of the Dutch coast (54°51' N, 4°44' E) (van der Laan-  
14 Luijkx et al., 2010) are compared to hourly modelled averages (Fig. 5) during the six year simulated  
15 period. This results in a correlation of 0.64, and a RMSE of 5.7 ppm. Local sources can influence  
16 the measured CO<sub>2</sub> concentration under certain wind conditions at F3. Consequently, the most  
17 extreme outliers were filtered out with the help of simultaneous CH<sub>4</sub> and CO measurements, when  
18 the influence from the local source was obvious. Continuous measurements at F3 conducted in a  
19 previous study (van der Laan-Luijkx et al., 2010) and covering a shorter period have indicated that  
20 the diurnal variation in the CO<sub>2</sub> concentration at this marine site F3 is negligible. Day to day  
21 variations related to synoptic changes in the wind direction etc. is according to van der Laan-Luijkx  
22 and colleagues seen in the continuous data. This pattern is captured by the DEHM model. Thus, the  
23 underestimation of the diurnal cycle by DEHM over land (as seen at LUT and OST), might only  
24 affect the current study at the near coastal areas, whereas CO<sub>2</sub> concentrations simulated by DEHM  
25 over open waters are more representable

26 As to examine the model performance on a longer time scale, weekly averages are made for the two  
27 marine stations Mace Head, Ireland (MHD, 53°20' N, 9°54' W) (Biraud et al., 2000) and Westerland,  
28 Germany (WES, 54°56' N, 8°19' E) (UBA, 2014), and the remote continental station, Pallas-  
29 Sammaltunturi, Finland (PAL, 67°58' N, 24°07' E) (FMI, 2013) for the six year period (Fig. 5). In  
30 general a reasonable correspondence between model and observations is seen during this period  
31 with correlations of 0.96, 0.98 and 0.89, and RMSEs of 1.8 ppm, 1.9 ppm and 3.8 ppm for MHD,

1 PAL and WES, respectively. The ability of the model to capture the seasonal cycle contributes to  
2 the very high correlation, but the model is also capable of capturing weekly variability and transport  
3 events especially during winter.

4 To conclude, this evaluation shows that the DEHM model captures the overall atmospheric CO<sub>2</sub>  
5 pattern across the marine region in focus in the current study.

## 6 **3.2 Air-sea CO<sub>2</sub> fluxes**

7 In order to investigate the effect of short variability in atmospheric CO<sub>2</sub> concentrations on the air-  
8 sea CO<sub>2</sub> flux, two different model simulations are conducted. One model simulation has  
9 atmospheric CO<sub>2</sub> concentrations that vary from time step to time step according to the fluxes and  
10 atmospheric transport in DEHM. This is in the following referred to as the VAT ('Variable  
11 ATmosphere') simulation. The other simulation contains at each time step and grid cell the monthly  
12 mean CO<sub>2</sub> concentration for the given month. This is in the following referred to as CAT ('Constant  
13 ATmosphere'). All other settings are identical in the two simulations. The simulations are made for  
14 the period 2005 to 2010 using the transfer velocity parameterisation by W92.

15 First, the results of atmospheric CO<sub>2</sub> concentrations and air-sea CO<sub>2</sub> fluxes from the VAT  
16 simulation will be presented. These results can be used to get an understanding of how the  
17 atmospheric CO<sub>2</sub> concentrations vary, and of how the air-sea CO<sub>2</sub> fluxes behave in terms of size  
18 and direction in the different sub-basins of the Baltic Sea and Danish inner waters. This will be  
19 followed by the comparison of the VAT and CAT simulation.

### 20 **3.2.1 Variable atmospheric CO<sub>2</sub> concentration**

21 The variability of atmospheric CO<sub>2</sub> in the Baltic area is illustrated in Fig. 6, which shows a few  
22 examples of the hourly simulated surface concentration. The top panel shows the variability in  
23 February 2007, where synoptic scale variability influence transport of CO<sub>2</sub>, and hence the surface  
24 concentrations. On 1 February 2007 at 4 GMT, a low pressure system has during the last days  
25 moved through Southern Scandinavia and is now located over Poland. This system has rotated  
26 continental air with high levels of CO<sub>2</sub> from the east towards the Baltic Sea. On 3 February 2007,  
27 the prevailing winds are now westerly, where marine air masses with lower CO<sub>2</sub> concentrations are  
28 transported towards the Baltic Sea. The lower panel of Fig. 6 shows the diurnal variability on 14  
29 July 2007. At 2 GMT, air masses with high CO<sub>2</sub> concentrations are transported from land towards

1 the marine areas – most evident in near-coastal areas. The same is the case at 14 GMT, but with  
2 lower concentrations due to extensive atmospheric mixing (a deep atmospheric boundary layer) and  
3 the uptake of CO<sub>2</sub> by the terrestrial biosphere at this time of the day. These examples show that  
4 large spatial gradients of up to 20 ppm can develop across the Baltic Sea during summer.

5 The seasonal averaged air-sea CO<sub>2</sub> fluxes estimated by DEHM in the VAT simulation are shown in  
6 Fig. 3.b. In winter, a gradient is seen from the North Sea through the Danish inner straits towards  
7 the Baltic Sea, indicating a large release of CO<sub>2</sub> to the atmosphere in the Baltic, and uptake in the  
8 North Sea. Progressing to spring, the gradient towards the Baltic ceases and all areas now have  
9 marine uptake of atmospheric CO<sub>2</sub>, which continues throughout the summer. In fall, the gradient  
10 starts to build up again, and the Baltic Sea becomes a source of CO<sub>2</sub> to the atmosphere.

11 The monthly mean 2005-2010 sub-basin averaged fluxes likewise depict this seasonality (Fig. 7).  
12 The highest seasonal amplitudes are found in the Baltic Sea area stretching from the Baltic Proper  
13 and northwards with the greatest seasonal amplitude of 12 gC m<sup>-2</sup> month<sup>-1</sup> found in the Bothnain  
14 Sea. Less seasonal variation in the CO<sub>2</sub> flux is obtained for Kattegat and the Danish Straits, which  
15 yearly experiences a variability of just 4.3 g C m<sup>-2</sup> month<sup>-1</sup>.

16 The total sub-basin monthly mean fluxes of CO<sub>2</sub> between the atmosphere and ocean show a  
17 seasonal variation for all areas with release in winter and uptake of atmospheric CO<sub>2</sub> in summer  
18 (Table 1). The entire area comprising of the six sub-basins has for the period 2005-2010 an average  
19 annual net uptake of atmospheric CO<sub>2</sub> of 287 Gg C yr<sup>-1</sup>. However, the net exchange varies greatly  
20 from sub-basin to sub-basin. Kattegat, the Western Baltic Sea and the Baltic Proper all have annual  
21 net uptake of atmospheric CO<sub>2</sub> averaged over 2005 to 2010, while the remaining three sub-basins  
22 release CO<sub>2</sub> to the atmosphere. The Baltic Proper contributes the most to the total annual averaged  
23 flux with an uptake of 254 g C yr<sup>-1</sup>, but during the individual months the fluxes in the Baltic Proper  
24 are even larger (up to 900 g C month<sup>-1</sup>). Monthly fluxes of this considerable size are not obtained in  
25 any of the other sub-domains. This is of course related to the fact that the Baltic Proper has the  
26 greatest spatial extent of all the six sub-basins.

27 To estimate the marine contribution in the Danish national CO<sub>2</sub> budget, the air-sea CO<sub>2</sub> flux in the  
28 Danish Exclusive Economic Zone (EEZ) is calculated. The EEZ is a zone adjacent to the territorial  
29 waters extending up to 200 nautical mile off shore, and in the EEZ the coastal state has the right to  
30 explore, exploit and manage all resources within this area (United Nations Chapter XXI Law of the  
31 Sea, 1984). The Danish EEZ has an area of approximately 105.000 km<sup>2</sup> (Fig. S2 in the Supp.

1 Material). During the six years simulated an average annual uptake in the Danish EEZ of 2613 Gg  
2 C yr<sup>-1</sup> is obtained. Here, the annual average of 2616 Gg C yr<sup>-1</sup> is reported. The inter-annual  
3 variability of the estimated flux will solely be a result of the inter-annual variations in the  
4 atmospheric CO<sub>2</sub>, as a climatology is used for the surface water  $p\text{CO}_2^w$ , due to the limited amount of  
5 data. The main part of the uptake in the Danish EEZ occurs in the North Sea. The North Sea has the  
6 largest extent in the Danish EEZ and combined with a small seasonal amplitude in  $p\text{CO}_2^w$ , this  
7 results in a constant uptake throughout the year. The other sub-basins within the Danish EEZ all  
8 release CO<sub>2</sub> in winter and take up CO<sub>2</sub> during summer. Compared to the Danish national emissions  
9 of anthropogenic CO<sub>2</sub>, the marine uptake by the Danish EEZ corresponds to 18 % per year of these  
10 emissions (Table 2). For the six year period investigated, the annual mean inventory in CO<sub>2</sub>  
11 excluding land use and land use change is 14.6 Tg C (Nielsen et al., 2013).

### 12 3.2.2 Constant Atmospheric CO<sub>2</sub> concentration

13 The impact of variations in the atmospheric CO<sub>2</sub> concentration is analysed in the following by  
14 comparing the results of the air-sea CO<sub>2</sub> fluxes for the VAT and CAT simulations in the six sub-  
15 basins. A total annual difference of 184 Gg C yr<sup>-1</sup> is obtained, which corresponds to a 64 %  
16 difference (calculated with VAT as the reference). CAT gives a total annual uptake of 471 Gg C yr<sup>-1</sup>,  
17 while VAT only has an annual uptake of 287 Gg C yr<sup>-1</sup>. The seasonal difference between VAT  
18 and CAT across the study area is seen in Fig. 8. The monthly fluxes in the sub-basins maintain the  
19 same direction in both VAT and CAT. However, for months where the different sub-basins  
20 experience outgassing, the outgassing is reduced in the CAT simulation as compared to in the VAT  
21 simulation. For months with uptake of CO<sub>2</sub> in the individual sub-basins, a higher uptake is  
22 simulated with the CAT setup than with the VAT setup.

23 In order to further analyse the difference between the VAT and the CAT simulations, times series of  
24 the driving parameters are compared. Examples of the atmospheric  $p\text{CO}_2$  ( $p\text{CO}_2^a$ ) in the lowest  
25 model layer in the VAT and CAT simulations are shown for a coastal site south of Sweden (55°18'  
26 N, 13°55' E) in Fig. 9 and 10 for February and July 2007, respectively. This site is chosen, as it can  
27 be influence by air masses from both land and sea depending on the wind direction.

28 February represents a case of outgassing, and July a case of marine uptake of atmospheric CO<sub>2</sub>.  
29 Time series of wind velocity at 10 meters,  $u_{10}$ , and the atmospheric mixing height,  $h_{\text{mix}}$ , are also  
30 plotted, as to get indications of horizontal transport and vertical mixing. In addition, the differences



1 in the atmospheric partial pressure of CO<sub>2</sub> ( $\Delta p\text{CO}_2^a$ ) and in the air-sea CO<sub>2</sub> flux ( $\Delta F_{\text{CO}_2}$ ) between  
2 the two simulations are shown (calculated as VAT – CAT). Differences in the  $p\text{CO}_2^a$  in the two  
3 simulations determine the difference in  $\Delta p\text{CO}_2$  between the two simulations, as the partial pressure  
4 of CO<sub>2</sub> in the water is the same in the two simulations.  $p\text{CO}_2^a$  is the only variable allowed to vary in  
5 the air-sea CO<sub>2</sub> flux calculations between VAT and CAT, and is thus responsible for the obtained  
6 flux difference.

7 For both months  $p\text{CO}_2^a_{\text{VAT}}$  fluctuates around the constant  $p\text{CO}_2^a_{\text{CAT}}$ . During the first half of  
8 February, a period of anti-correlation between  $p\text{CO}_2^a_{\text{VAT}}$  and  $u_{10}$  is seen. This anti-correlation is  
9 greatest during the second week with a weekly correlation coefficient ( $r$ ) equal to -0.69. Thus, for  
10 this period the episodes of high wind speed tend to dilute the  $p\text{CO}_2^a$  levels allowing for a greater  
11  $\Delta p\text{CO}_2$  in the VAT simulation than in the CAT simulation. During the last week of February, a  
12 positive correlation of  $r = 0.62$  between the two parameters is obtained with wind speeds above 10  
13  $\text{m s}^{-1}$  and high  $p\text{CO}_2^a$  levels in the atmosphere. This gives smaller  $\Delta p\text{CO}_2$  in the VAT simulation  
14 than in the CAT simulation, which results in greater fluxes in the CAT simulation. In February no  
15 clear diurnal cycle is seen in the mixing height, but the mixing height seems to follow the pattern of  
16 the wind speed with decreases in  $h_{\text{mix}}$  during periods with low wind speeds and increases in  $h_{\text{mix}}$   
17 during high wind speeds. The correlation between these two parameters in February is  $r = 0.72$ .  
18 Hence, in February the  $p\text{CO}_2^a_{\text{VAT}}$  levels are dominated by horizontal transport.

19 In July a clear diurnal variability is seen in  $p\text{CO}_2^a_{\text{VAT}}$ , and an anti-correlation between  $h_{\text{mix}}$  and  
20  $p\text{CO}_2^a_{\text{VAT}}$  is evident throughout the month with the highest anti-correlation during the last week  
21 (with  $r = -0.72$ ). During July the so-called diurnal rectifier effect is modelled by the VAT  
22 simulation. The rectifier effect is most apparent during the growing season and can be described as  
23 the collaboration between terrestrial ecosystems and boundary layer dynamics that act towards  
24 lowering  $p\text{CO}_2^a$  during the day and increase it during night (Denning et al., 1996). Due to the  
25 constant level of atmosphere CO<sub>2</sub> in the CAT simulation, the rectifier effect is absent here. This  
26 results in a greater uptake of atmospheric CO<sub>2</sub> in the CAT simulation than the VAT simulation  
27 during the growing season.

28 An anti-correlation between  $\Delta p\text{CO}_2^a$  and  $\Delta F_{\text{CO}_2}$  is seen in both February and July. During winter the  
29 largest difference in the air-sea CO<sub>2</sub> flux between VAT and CAT coincides with high wind speeds  
30 or large differences in the atmospheric CO<sub>2</sub> concentrations (hence large  $\Delta p\text{CO}_2^a$  values). In summer  
31 the diurnal cycle in the atmospheric CO<sub>2</sub> levels are translated into the flux difference.

1 Vertical profiles of atmospheric CO<sub>2</sub> at the site south of Sweden have been plotted together with  
2 h<sub>mix</sub> in Fig. 11. Note that the unit in Fig. 11 is ppm and not µatm. The variability of CO<sub>2</sub> is also  
3 evident in the vertical profile, where air masses with low or high CO<sub>2</sub> concentrations are being  
4 transported to and from the site (55°18'N, 13°55'E). Continental air is represented by high levels of  
5 CO<sub>2</sub> that extend up to 2 km into the atmosphere, while marine air masses have lower levels of CO<sub>2</sub>  
6 corresponding to the levels above 2 km. The shift between the two types of air masses is clearly  
7 seen in the vertical profile e.g. on 2 February. Here higher wind speed leads to transport of marine  
8 air masses to the site (see Fig. 9). Like Fig. 9, the vertical profile in February shows no clear  
9 connection between surface concentrations of CO<sub>2</sub> and h<sub>mix</sub>. In July, the vertical profile depicts the  
10 rectifier effect. Low surface values of CO<sub>2</sub> coincide with the greatest boundary layer heights found  
11 during the day time, and high surface levels of CO<sub>2</sub> concur during night time with the nocturnal  
12 boundary layer. It is remarkable how the vertical profile during July 2007 represents a much more  
13 mixed atmosphere as compared to February 2007, where the marine and continental air masses  
14 clearly are distinguished from each other.

15

## 16 **4 Discussion**

### 17 **4.1 Surface water pCO<sub>2</sub><sup>w</sup> climatology**

18 A representative map of surface pCO<sub>2</sub><sup>w</sup> has been created for Skagerrak and six sub-domains in the  
19 Baltic using two data sets, one obtained from monitoring stations and one using underway  
20 measurements of surface pCO<sub>2</sub><sup>w</sup> (see Sect. 2.2).

21 Previous estimates of pCO<sub>2</sub><sup>w</sup> at two positions within the Baltic Sea have shown an inter-annual  
22 variability of up to 25 % in winter and almost 140 % in summer (Wesslander et al., 2010).  
23 Likewise, large short term variability has been measured in different coastal systems (Dai et al.,  
24 2009; Leinweber et al., 2009; Wesslander et al., 2011).

25 The representation of surface pCO<sub>2</sub><sup>w</sup> values in the sub-domains by a monthly averaged value does  
26 not account for the temporal variability during each month and the spatial variability in the  
27 relatively large areas. The estimated surface fields of pCO<sub>2</sub><sup>w</sup> are based on all available data,  
28 however, the amount of available observations can be considered to be relatively small compared  
29 to the large study area - although, underway pCO<sub>2</sub><sup>w</sup> measurements (Schneider and Sadkowiak, 2012)  
30 have increased the data coverage in the central Baltic Sea significantly in the most recent years.

1 The choice of applying surface map of  $p\text{CO}_2^w$  for six domains in the Baltic of course introduces  
2 some biases on the flux estimates, as mechanisms, such as upwelling and algae blooms that act on a  
3 smaller spatial scale than the sub-division are not specifically accounted for. It was essential for the  
4 present study to obtain a surface map of  $p\text{CO}_2^w$  that covered the entire region, as to be able to study  
5 the effect of short term variability in atmospheric  $\text{CO}_2$  on the air-sea  $\text{CO}_2$  flux within the Baltic Sea  
6 region. Despite the possible biases of ignoring short term and small scale variability in ocean  
7  $p\text{CO}_2^w$ , the simplified description of the conditions in the Baltic Sea in a number of sub-domains  
8 was evaluated to be the best solution in order to obtain a surface field of  $p\text{CO}_2^w$  that spatially covers  
9 the whole model domain for the present study.

## 10 **4.2 Air-sea $\text{CO}_2$ fluxes**

11 The atmospheric  $\text{CO}_2$  concentration is seen to vary greatly within the study area (Fig. 6 and 11). The  
12 dynamics of the fluxes and the atmospheric transport and mixing lead to short-term variations and  
13 spatial gradients in the atmospheric  $\text{CO}_2$  level across the study area. Pressure systems move through  
14 the region transporting air masses with different characteristics and  $\text{CO}_2$  levels to and from the  
15 Baltic and the Danish inner waters. In the growing season, the effect from the terrestrial biosphere is  
16 apparent with a clear diurnal cycle in the atmospheric  $\text{CO}_2$  caused by respiration during night time  
17 and photosynthesis during the day complemented by boundary layer dynamics. Even these short  
18 term variations in atmospheric  $\text{CO}_2$  concentrations over land can be transported to marine areas,  
19 indicating why atmospheric short term variability is important to include in the air-sea flux  
20 estimations.

21 For the six year period an annual average uptake of  $287 \text{ Gg C yr}^{-1}$  is obtained with the VAT-setup as  
22 a total for the six sub-basins. A statistical analysis of the simulated fluxes shows that Kattegat and  
23 the Western Baltic Sea are annual sinks (at a significance level of 0.05), while the Gulf of Finland  
24 and the Bay of Bothnia are annual sources of atmospheric  $\text{CO}_2$ . In the transition zone between  
25 these areas, i.e. the Baltic Proper and the Bothnian Sea, large variations in the annual flux are seen  
26 in this study. During the six years simulated these sub-domains change annually between being  
27 sources and sinks of  $\text{CO}_2$  to the atmosphere. This also affects the total flux for the entire  
28 investigated area, which also shifts between being an annual source ( $376 \text{ Gg C yr}^{-1}$ ) and sink ( $-1100$   
29  $\text{Gg C yr}^{-1}$ ). A significant test (student's t-test with a significance level of 0.05) show that the

1 variability from year to year during the six years simulated is so large that we cannot conclude that  
2 the area is a net sink, despite the estimated averaged uptake of 287 Gg C yr<sup>-1</sup>.

3 The air-sea CO<sub>2</sub> fluxes obtained from the VAT simulation for six sub-basins are compared to  
4 previous results from the area to assess the consistency. Previous studies of the air-sea CO<sub>2</sub> flux in  
5 the Baltic Sea area are ambiguous as to the Baltic Sea's role in the carbon cycle (see Table 3). This  
6 is partly caused by the various techniques used, ranging from in-situ measurements using the eddy  
7 covariance method to model simulations (Kulinski and Pempkowiak, 2011; Rutgersson et al., 2009;  
8 Weiss et al., 2007; Wesslander et al., 2010), and partly by the different spatial areas investigated.  
9 Some of the previous studies are site specific (Algesten et al., 2006; Kuss et al., 2006; Löffler et al.,  
10 2012; Rutgersson et al., 2008; Wesslander et al., 2010), and other studies cover the entire area  
11 (Gustafsson et al., 2014; Kulinski and Pempkowiak, 2011; Norman et al., 2013). None of the  
12 previous regional studies have based their estimates of the air-sea CO<sub>2</sub> flux on results from an  
13 atmospheric transport model capable of combining large spatial coverage with high spatiotemporal  
14 resolution of the entire Baltic region as in the present study. Results from previous studies and the  
15 present study have been converted to the same unit of g C m<sup>-2</sup> yr<sup>-1</sup>, as to allow for a direct  
16 comparison (Table 3).

17 Table 3 reveals that in terms of the direction of the flux, the present study corresponds well with  
18 some of the previous studies and contradicts others. As the results obtained from the VAT  
19 simulation lie within the range of previous estimates, it seems reasonable to use the current model  
20 setup for sensitivity analysis of the air-sea CO<sub>2</sub> flux in the region. Additionally, it can be concluded  
21 that the obtained results from the VAT simulation together with recent studies converge towards the  
22 Baltic Sea and the Danish inner waters being annual sinks of atmospheric CO<sub>2</sub>.

### 23 **4.3 Impact of atmospheric short term variability**

24 The difference of 184 Gg C yr<sup>-1</sup> between the annual air-sea flux in the CAT and VAT simulations  
25 was tested to be significantly different from zero at a 0.05 significance level. Therefore, it can be  
26 concluded that using a constant level of atmospheric CO<sub>2</sub> has a significant impact on the estimated  
27 annual air-sea CO<sub>2</sub> flux in this region. The greatest differences are found in winter and fall in the  
28 Baltic Sea area (Fig. 8). But large differences are also found over open water areas in spite of a less  
29 variable atmospheric CO<sub>2</sub> concentration here, i.e. a smaller difference in the atmospheric CO<sub>2</sub>  
30 concentration between the two simulations. Despite the small concentration difference, the tendency

1 to higher wind speeds over open oceans leads to the large flux difference here. The same wind  
2 fields are applied in both simulations.

3 The deviation between the two simulations in the study region is mainly caused by a reduction in  
4 the winter uptake in the CAT simulation. The winter outgassing is reduced in CAT, when the  $p\text{CO}_2^a$   
5 of the CAT is greater than the  $p\text{CO}_2^a$  of the VAT simulation. Thereby,  $\Delta p\text{CO}_2$  is smaller in the  
6 CAT simulation than the VAT simulation, and the flux will be reduced. Furthermore, the  
7 nonlinearity of the wind speed in the parameterisation of the transfer velocity can amplify this  
8 reduction, in particular, when high wind speeds coincide with greater  $\Delta p\text{CO}_2$  in the VAT simulation  
9 than in CAT simulation (e.g. as seen in Fig.9 first week of February 2007). This mechanism must  
10 have a significant influence, as it results in a greater winter uptake in the VAT simulation than in  
11 the CAT simulation.

12 The higher marine  $\text{CO}_2$  uptake in summer by the CAT simulation is a result of diurnal boundary  
13 layer dynamics and the diurnal cycle or lack of it in the atmospheric  $\text{CO}_2$  concentrations. The  
14 rectifier effect is not accounted for in the CAT simulation, and the constant  $p\text{CO}_2^a$  in CAT is higher  
15 during the day and lower during the night than in the VAT simulation. This allows for a greater air-  
16 sea  $\Delta p\text{CO}_2$  in the CAT simulation during day, which together with a tendency of higher wind speeds  
17 during day time increases the oceanic uptake in CAT. This is illustrated by  $\Delta F_{\text{CO}_2}$ , where positive  
18 values indicate how the flux is numerical larger in CAT than VAT (see Fig. 10). As described in  
19 Sect. 3.1, the diurnal cycle of atmospheric  $\text{CO}_2$  is generally underestimated by the DEHM model in  
20 near coastal areas. This could indicate that the difference between the VAT and CAT simulations  
21 found during the growing season is a conservative estimate for the fluxes at the near coastal areas in  
22 the Baltic Sea region.

23 While Rutgersson et al. (2008) found a slightly overestimated seasonal amplitude, when using a  
24 constant atmospheric  $\text{CO}_2$  concentration, the present study finds that the seasonal cycle of the CAT  
25 simulation is displaced downwards as compared to the VAT simulation. This displacement results  
26 in a greater annual uptake in the CAT simulation.

#### 27 **4.4 Uncertainties**

28 The estimated air-sea  $\text{CO}_2$  flux is controlled by several parameters in the applied model setup:  
29 choice of transfer velocity parameterisation, wind speed, temperature, salinity, atmospheric  $\text{CO}_2$   
30 concentration and marine  $p\text{CO}_2^w$  surface values. Each of these is connected with some uncertainty

1 and errors.

2 Takahashi et al. (2009) estimate the combined precision on the global air-sea flux to be on the order  
3 of  $\pm 60\%$ , when including a possible climatology bias due to interpolation and under-sampling. The  
4 uncertainty might be higher in the current study, as the climatology for the  $p\text{CO}_2^w$  in surface waters  
5 used here covers areas where the spatiotemporal variability in the measured  $p\text{CO}_2^w$  is higher than in  
6 open waters. The natural variability within the sub-domains is represented by the standard  
7 deviations in Fig. 2 and it reflects both the spatial and temporal variation in the domains during the  
8 period of sampling, i.e. the last decade. The Baltic Sea domains (i.e. except the Kattegat sub-  
9 domain) are all characterised by a significant under-saturation of the surface water during spring  
10 and summer. During winter these stations are in general supersaturated with respect to the  
11 atmospheric  $p\text{CO}_2^a$ . Thus, the sign of the  $\text{CO}_2$  flux during the seasons is assumed to be well-  
12 determined in the Baltic Sea sub-domains due to the large seasonal amplitudes. However, during the  
13 seasonal change between summer and winter, where typical standard deviations in the climatology  
14 of 50 ppm are seen, we estimate that the uncertainty due to the ocean surface  $p\text{CO}_2^w$  values is in the  
15 order of 50 % in the Baltic Sea. The uncertainty in the Kattegat sub-domain is estimated to be up to  
16 50 - 100% because of the relatively small seasonal amplitude.

17 Atmospheric  $\text{CO}_2$ , wind speed and temperature all vary in each model time step and grid cell. The  
18 uncertainties of wind speed and temperature are small compared to the uncertainties of the  $p\text{CO}_2^w$   
19 fields. Fig. 4 and Fig. 5 show how well the DEHM model captures the weekly and seasonal  
20 variability in the atmospheric  $\text{CO}_2$  concentrations. However, some problems arise in capturing the  
21 variability on shorter time scales (e.g. diurnal). The diurnal cycle is under-estimated in this model  
22 setup, which is related to the coarse resolution of the biosphere fluxes, and of the model itself.

23 Short term variability does not only exist in the atmospheric concentration of  $\text{CO}_2$ , it has also been  
24 detected in the  $p\text{CO}_2^w$  of surface water (Dai et al., 2009; Leinweber et al., 2009; Rutgersson et al.,  
25 2008; Wesslander et al., 2011). The magnitude of the short term variability is site dependent with  
26 smallest variability found in open oceans (Dai et al., 2009) and greatest at near-coastal sites  
27 (Leinweber et al., 2009; Wesslander et al., 2011). Off the Californian coast, Leinweber et al. (2009)  
28 find a diurnal cycle of  $p\text{CO}_2^w$  with an average amplitude of 20  $\mu\text{atm}$  - a diurnal amplitude double of  
29 what they find in the atmosphere. Short term variability of marine  $p\text{CO}_2^w$ , could potentially alter the  
30 annual estimate of the coastal air-sea  $\text{CO}_2$  flux. Thus, in the present study the fluxes at the near-  
31 coastal areas within the sub-domain could be affected by this short term variability, and as a result

1 possibly modify the total flux for these sub-domains. However, the short term variability in marine  
2  $p\text{CO}_2^w$  is not included in this study, and it is, therefore, difficult to estimate how this might affect the  
3 estimated flux. Additionally, the short term variability in the air and water might be correlated, thus  
4 it is not possible to make a deduction of the combined effect in the present model study.

5 As to assess the uncertainty connected to the choice of transfer velocity on the estimated air-sea flux  
6 model, simulations using parameterisations of Nightingale et al. (2000) and Weiss et al. (2007) have  
7 also been conducted. Throughout the seasons the parameterisation by Weiss et al. (2007) gives  
8 more extreme values than Nightingale et al. (2000), but the annual sum for the study area results in -  
9 667 and -858 Gg C yr<sup>-1</sup> for Nightingale et al. (2000) and Weiss et al. (2007), respectively. Other  
10 transfer velocity parameterisations could also have been interesting to use in the presents study. An  
11 example is the parameterisation by Sweeney et al. (2007), which is based on an updated and  
12 improved version of the radiocarbon method used in W92. Here, the two different parameterisations  
13 by Weiss et al. (2007) and Nightingale et al. (2000) were chosen, as these experiments were  
14 conducted within and close to the study area, respectively.

15 The present study supports the findings briefly touched upon by Rutgersson et al. (2009), who  
16 conclude that the uncertainty due to the value of atmospheric CO<sub>2</sub> is small compared to uncertainty  
17 in transfer velocity. Introducing a surface  $p\text{CO}_2^w$  climatology in six sub-basins adds substantial to the  
18 uncertainty, as short term variability in both space and time is ignored in this parameter. However,  
19 we have chosen to use this surface  $p\text{CO}_2^w$  climatology, as to get full spatial and temporal coverage  
20 of surface  $p\text{CO}_2^w$ . This allows us to investigate the effect of short term variability in atmospheric  
21 CO<sub>2</sub> concentration on the air- sea CO<sub>2</sub> flux.

## 22 **5 Conclusion**

23 Using an atmospheric CO<sub>2</sub> model with a relative high spatial and temporal resolution we have  
24 estimated the air-sea flux of CO<sub>2</sub> in the Danish inner waters and the Baltic Sea region. More  
25 specifically we have made a detailed analysis of the sensitivity to temporal variability in  
26 atmospheric CO<sub>2</sub> and the related impact of driving parameters like wind speed and atmospheric  
27 mixing height.

28 In the process of this study new monthly marine  $p\text{CO}_2^w$  fields have been developed for the region  
29 combining existing data from monitoring stations and measurements from ships. Due to the  
30 sparseness of these data, only seasonal variations are included in the  $p\text{CO}_2^w$  fields.

1 The atmospheric concentration of CO<sub>2</sub> is often assumed to be constant or only vary by season in  
2 many marine model studies, but according to this novel sensitivity analysis, neglecting e.g. the  
3 diurnal and synoptic variability in atmospheric CO<sub>2</sub> concentrations could lead to a systematic bias  
4 in the annual net air-sea flux. Previous studies have looked at the entire Baltic region (Gustafsson et  
5 al., 2014; Kulinski and Pempkowiak, 2011; Norman et al., 2013; Thomas and Schneider, 1999), but  
6 not with the same approach as in the present study.

7 In all the included sub-basins a seasonal cycle was detected in the air-sea CO<sub>2</sub> flux with release of  
8 CO<sub>2</sub> during winter and fall, and uptake of atmospheric CO<sub>2</sub> in the remaining months. An annual  
9 flux for the study area of -287 Gg C yr<sup>-1</sup> (-0.7 g C m<sup>2</sup> yr<sup>-1</sup>) was obtained for the six years simulated.  
10 This agrees with the previous findings of Norman et al. (2013) and Gustafsson et al. (2014), who  
11 estimate annual air-sea CO<sub>2</sub> fluxes of -2.6 g C m<sup>2</sup> yr<sup>-1</sup> and -4.3 g C m<sup>2</sup> yr<sup>-1</sup>, respectively.

12 The importance of short term variations in the atmospheric CO<sub>2</sub> in relation to the yearly air-sea flux  
13 was tested with two different model simulations. One simulation includes the short-term variations  
14 (the VAT simulation), while the other simulation includes a monthly constant atmospheric CO<sub>2</sub>  
15 concentration (the CAT simulation). A significant difference of 184 Gg C yr<sup>-1</sup> (corresponding to 67  
16 %) was obtained for the air-sea CO<sub>2</sub> flux for the Baltic Sea and Danish inner waters between the  
17 two model simulations. The seasonal amplitude of the air-sea CO<sub>2</sub> flux was in the CAT simulation  
18 shifted downwards as compared to the VAT simulation, resulting in a reduced winter release of CO<sub>2</sub>  
19 in the CAT simulation and an increased summer uptake. The difference occurs solely due to the  
20 difference in the atmospheric CO<sub>2</sub> concentrations.

21 As a part of the Danish project ECOCLIM with focus on the Danish CO<sub>2</sub> budget, the natural marine  
22 annual flux of CO<sub>2</sub> was for the first time estimated in the present study. The Danish waters - in this  
23 context defined as the Danish Exclusive Economic Zone - is according to our simulations taking up  
24 2613 Gg C yr<sup>-1</sup> with the majority taken up in the North Sea. This is comparable to approximately  
25 18% of the Danish anthropogenic CO<sub>2</sub> emissions.

26 Uncertainties are bound to the results in particularly in connection with transfer velocity  
27 parameterisation and the applied surface pCO<sub>2</sub><sup>w</sup> climatology. However, in the present study with the  
28 two model simulations that only differ in the atmosphere CO<sub>2</sub> concentration, a distinguishable  
29 difference in the air-sea CO<sub>2</sub> flux is obtained. This, therefore, stresses the importance of including  
30 short term variability in the atmospheric CO<sub>2</sub> in order to minimise the uncertainties in the air-sea



1 CO<sub>2</sub> flux. Moreover, this deduce that also short term variability in  $p\text{CO}_2^w$  of the water, in particular  
2 of coastal areas, needs to be included, as short term variability in near coastal surface water  $p\text{CO}_2^w$   
3 potentially is greater than in the atmosphere.

4 To conclude, we recommend that future studies of the air-sea CO<sub>2</sub> exchange include short term  
5 variability of CO<sub>2</sub> in the atmosphere. Thereby, the uncertainty related to estimating the marine part  
6 of the carbon budget at regional to global scales can be reduced.

7

## 8 **Acknowledgements**

9 This study is a part of a PhD project within ECOCLIM founded by the Danish Strategic Research  
10 Council (grant number 10-093901). Further, several scientists involved with this work are likewise  
11 connected to the Nordic Centre of Excellence, DEFROST. We are grateful to Anna Rutgersson at  
12 Uppsala University for sharing atmospheric measurements of CO<sub>2</sub> at Östergarnsholm. We likewise  
13 thank the community for making observations available at Lutjewad, Mace Head, Pallas-  
14 Sammaltunturi and Westerland. We thank SMHI for sharing marine data from the six monitoring  
15 sites. Results from Carbon Tracker CT2011\_oi provided by NOAA ESRL, Boulder, Colorado, USA  
16 from the website at <http://carbontracker.noaa.gov> have contributed to this work, as have  
17 GLOBALVIEW-CO2, 2013 and European and Danish fossil fuel emission inventories from IER  
18 and Aarhus University, respectively. We are grateful for the very constructive comments from two  
19 anonymous reviewers.

20

## REFERENCES

- 1
- 2
- 3 Algesten, G., Brydsten, L., Jonsson, P., Kortelainen, P., Löfgren, S., Rahm, L., Räike, A., Sobek, S.,  
4 Tranvik, L., Wikner, J., and Jansson, M.: Organic carbon budget for the Gulf of Bothnia, *J. Marine*  
5 *Syst.*, 63, 155-161, 2006.
- 6 Bendtsen, J., Gustafsson, K. E., Söderkvist, J., and Hansen, J. L. S.: Ventilation of bottom water in  
7 the North Sea-Baltic Sea transition zone, *J. Marine Syst.*, 75, 138-149, 2009.
- 8 Biraud, S., Ciais, P., Ramonet, M., Simmonds, P., Kazan, V., Monfray, P., O'Doherty, S., Spain, T.  
9 G., and Jennings, S. G.: European greenhouse gas emissions estimated from continuous  
10 atmospheric measurements and radon 222 at Mace Head, Ireland, *J. of Geophys. Res. -Atmos*, 105,  
11 1351-1366, 2000.
- 12 Boden, T. A., Marland, G., and Andres, R. J.: Global, Regional, and National Fossil-Fuel CO<sub>2</sub>  
13 Emissions, Carbon Dioxide Information Analysis Center, Oak Ridge National Laboratory, U. S.  
14 Department of Energy, Oak Ridge, Tenn. , U. S. A., 2013.
- 15 Borges, A. V., Schiettecatte, L. S., Abril, G., Delille, B., and Gazeau, E.: Carbon dioxide in  
16 European coastal waters, *Estuar. Coast. Shelf S.*, 70, 375-387, 2006.
- 17 Boyer, T., Levitus, S., Garcia, H., Locarnini, R. A., Stephens, C., and Antonov, J.: Objective  
18 analyses of annual, seasonal, and monthly temperature and salinity for the world ocean on a 0.25  
19 degrees grid, *Int. J. Climatol.*, 25, 931-945, 2005.
- 20 Brandt, J., Silver, J. D., Frohn, L. M., Geels, C., Gross, A., Hansen, A. B., Hansen, K. M.,  
21 Hedegaard, G. B., Skjøth, C. A., Villadsen, H., Zare, A., and Christensen, J. H.: An integrated  
22 model study for Europe and North America using the Danish Eulerian Hemispheric Model with  
23 focus on intercontinental transport of air pollution, *Atmos. Environ.*, 53, 156-176, 2012.
- 24 Cai, W. J.: Estuarine and Coastal Ocean Carbon Paradox: CO<sub>2</sub> Sinks or Sites of Terrestrial Carbon  
25 Incineration?, *Annu. Rev. Marine. Sci.*, 123-145, 2011.
- 26 CarbonTracker CT2011\_oi, <http://carbontracker.noaa.gov>, last access: 1 August 2013.

- 1 Chen, C. T. A. and Borges, A. V.: Reconciling opposing views on carbon cycling in the coastal  
2 ocean: Continental shelves as sinks and near-shore ecosystems as sources of atmospheric CO<sub>2</sub>,  
3 Deep-Sea Res. PT. II, 56, 578-590, 2009.
- 4 Chen, C. T. A., Huang, T. H., Chen, Y. C., Bai, Y., He, X., and Kang, Y.: Air-sea exchanges of CO<sub>2</sub>  
5 in the world's coastal seas, Biogeosciences, 10, 6509-6544, 2013.
- 6 Christensen, J. H.: The Danish Eulerian hemispheric model - A three-dimensional air pollution  
7 model used for the Arctic, Atmos. Environ., 31, 4169-4191, 1997.
- 8 Dai, M. H., Lu, Z. M., Zhai, W. D., Chen, B. S., Cao, Z. M., Zhou, K. B., Cai, W. J., and Chen, C.  
9 T. A.: Diurnal variations of surface seawater pCO<sub>2</sub> in contrasting coastal environments, Limnol and  
10 Oceanogr, 54, 735-745, 2009.
- 11 Denning, A. S., Randall, D. A., Collatz, G. J., and Sellers, P. J.: Simulations of terrestrial carbon  
12 metabolism and atmospheric CO<sub>2</sub> in a general circulation model .2. Simulated CO<sub>2</sub> concentrations,  
13 Tellus B, 48, 543-567, 1996.
- 14 FMI, Atmospheric CO<sub>2</sub> hourly concentration data, Pallas-Sammaltunturi - FMI, WMO World Data  
15 Centre for Greenhouse Gases, Japan Meteorol. Agency, Tokyo.
- 16 Garbe, C. S., Rutgersson, A., Boutin, J., de Leeuw, G., Delille, B., Fairall, C. W., Gruber, N., Hare,  
17 J., Ho, D. H., Johnson, M. T., Nightingale, P. D., Pettersson, H., Piskozub, J., Sahlee, E., Tsai, W.,  
18 Ward, B., Woolf, D. K., and Zappa, C. J.: Transfer Across the Air-Sea Interface, in: Ocean-  
19 Atmosphere Interactions of Gases and Particles: Liss, P. S. and Johnson, M. T., Eds., Springer Earth  
20 System Science, 55-111, 2014.
- 21 Gattuso, J. P., Frankignoulle, M., and Wollast, R.: Carbon and carbonate metabolism in coastal  
22 aquatic ecosystems, Annu. Rev. Ecol. Syst., 29, 405-434, 1998.
- 23 Geels, C., Christensen, J. H., Frohn, L. M., and Brandt, J.: Simulating spatiotemporal variations of  
24 atmospheric CO<sub>2</sub> using a nested hemispheric model, Phys. Chem. Earth., 27, 1495-1505, 2002.

- 1 Geels, C., Doney, S. C., Dargaville, R., Brandt, J., and Christensen, J. H.: Investigating the sources  
2 of synoptic variability in atmospheric CO<sub>2</sub> measurements over the Northern Hemisphere continents:  
3 a regional model study, *Tellus B*, 56, 35-50, 2004.
- 4 Geels, C., Gloor, M., Ciais, P., Bousquet, P., Peylin, P., Vermeulen, A. T., Dargaville, R., Aalto, T.,  
5 Brandt, J., Christensen, J. H., Frohn, L. M., Haszpra, L., Karstens, U., Rödenbeck, C., Ramonet, M.,  
6 Carboni, G., and Santaguida, R.: Comparing atmospheric transport models for future regional  
7 inversions over Europe - Part 1: Mapping the atmospheric CO<sub>2</sub> signals, *Atmos. Chem. Phys.*, 7,  
8 3461-3479, 2007.
- 9 Geels, C., Hansen, K. M., Christensen, J. H., Skjøth, C. A., Ellermann, T., Hedegaard, G. B., Hertel,  
10 O., Frohn, L. M., Gross, A., and Brandt, J.: Projected change in atmospheric nitrogen deposition to  
11 the Baltic Sea towards 2020, *Atmos. Chem. Phys.*, 12, 2615-2629, 2012.
- 12 Giglio, L., van der Werf, G. R., Randerson, J. T., Collatz, G. J., and Kasibhatla, P.: Global  
13 estimation of burned area using MODIS active fire observations, *Atmos. Chem. Phys.*, 6, 957-974,  
14 2006.
- 15 GLOBALVIEW-CO<sub>2</sub>, Cooperative Global Atmospheric Data Integration Project. 2013, updated  
16 annually. Multi-laboratory compilation of synchronized and gap-filled atmospheric carbon dioxide  
17 records for the period 1979-2012 (obspack\_co2\_1\_GLOBALVIEW-CO<sub>2</sub>\_2013\_v1.0.4\_2013-12-  
18 23). Compiled by NOAA Global Monitoring Division: Boulder, Colorado, U.S.A. Data product  
19 accessed at <http://dx.doi.org/10.3334/OBSPACK/1002>.
- 20 Grell, G. A., Dudhia, J., and Stauffer, D. R.: A Description of the Fifth-generation Penn  
21 State/NCAR Mesoscale Model (MM5), National Center for Atmospheric Research, Boulder,  
22 Colorado, USA., NCAR Technical Note NCAR/TN-398+STR., 1995.
- 23 Gustafsson, E., Deutsch, B., Gustafsson, B. G., Humborg, C., and Mörth, C. M.: Carbon cycling in  
24 the Baltic Sea - The fate of allochthonous organic carbon and its impact on air-sea CO<sub>2</sub> exchange, *J.*  
25 *Marine Syst.*, 129, 289-302, 2014.
- 26 Högström, U., Sahlée, E., Drennan, W. M., Kahma, K. K., Smedman, A. S., Johansson, C.,  
27 Pettersson, H., Rutgersson, A., Tuomi, L., Zhang, F., and Johansson, M.: Momentum fluxes and

- 1 wind gradients in the marine boundary layer - a multi-platform study, *Boreal Environ. Res.*, 13,  
2 475-502, 2008.
- 3 Körtzinger, A., Thomas, H., Schneider, B., Gronau, N., Mintrop, L., and Durr, H. H.: At sea  
4 intercomparison of two newly designed underway  $p\text{CO}_2$  systems - encouraging results, *Mar. Chem.*,  
5 52, 133-145, 1996.
- 6 Kulinski, K. and Pempkowiak, J.: The carbon budget of the Baltic Sea, *Biogeosciences*, 8, 3219-  
7 3230, 2011.
- 8 Kuss, J., Roeder, W., Wloost, K. P., and DeGrandpre, M. D.: Time-series of surface water  $\text{CO}_2$  and  
9 oxygen measurements on a platform in the central Arkona Sea (Baltic Sea): Seasonality of uptake  
10 and release, *Mar. Chem.*, 101, 220-232, 2006.
- 11 Langner, J., Andersson, C., and Engardt, M.: Atmospheric input of nitrogen to the Baltic Sea basin:  
12 present situation, variability due to meteorology and impact of climate change, *Boreal Environ.*  
13 *Res.*, 14, 226-237, 2009.
- 14 Laruelle, G. G., Durr, H. H., Slomp, C. P., and Borges, A. V.: Evaluation of sinks and sources of  
15  $\text{CO}_2$  in the global coastal ocean using a spatially-explicit typology of estuaries and continental  
16 shelves, *Geophys. Res. Lett.*, 37, 2010.
- 17 Le Quéré, C., Andres, R. J., Boden, T., Conway, T., Houghton, R. A., House, J. I., Marland, G.,  
18 Peters, G. P., van der Werf, G. R., Ahlström, A., Andrew, R. M., Bopp, L., Canadell, J. G., Ciais,  
19 P., Doney, S. C., Enright, C., Friedlingstein, P., Huntingford, C., Jain, A. K., Jourdain, C., Kato, E.,  
20 Keeling, R. F., Klein Goldewijk, K., Levis, S., Levy, P., Lomas, M., Poulter, B., Raupach, M. R.,  
21 Schwinger, J., Sitch, S., Stocker, B. D., Viovy, N., Zaehle, S., and Zeng, N.: The global carbon  
22 budget 1959–2011, *Earth System Science Data*, 165-185, 2013.
- 23 Leinweber, A., Gruber, N., Frenzel, H., Friederich, G. E., and Chavez, F. P.: Diurnal carbon cycling  
24 in the surface ocean and lower atmosphere of Santa Monica Bay, California, *Geophys. Res. Lett.*,  
25 36, 2009.
- 26 Löffler, A., Schneider, B., Perttila, M., and Rehder, G.: Air-sea  $\text{CO}_2$  exchange in the Gulf of  
27 Bothnia, Baltic Sea, *Cont. Shelf. Res.*, 37, 46-56, 2012.

1 Meesters, A. G. C. A., Tolk, L. F., Peters, W., Hutjes, R. W. A., Vellinga, O. S., Elbers, J. A.,  
2 Vermeulen, A. T., van der Laan, S., Neubert, R. E. M., Meijer, H. A. J., and Dolman, A. J.: Inverse  
3 carbon dioxide flux estimates for the Netherlands, *J. of Geophys. Res. -Atmos*, 117, 2012.

4 Mørk, E. T., Sørensen, L. L., Jensen, B., and Sejr, M. K.: Air-Sea CO<sub>2</sub> Gas Transfer Velocity in a  
5 Shallow Estuary, *Bound-Lay Meteorol*, 151, 119-138, 2014.

6 Nielsen, O.-K., Plejdrup, M. S., Winther, M., Nielsen, M., Gyldenkærne, S., Mikkelsen, M. H.,  
7 Albrektsen, R., Thomsen, M., Hjelgaard, K., Hoffmann, L., Fauser, P., Bruun, H. G., Johannsen, V.  
8 K., Nord-Larsen, T., Vesterdal, L., Møller, I. S., Caspersen, O. H., Rasmussen, E., Petersen, S. B.,  
9 Baunbæk, L., and Hansen, M. G.: Denmark's National Inventory Report 2013. Emission Inventories  
10 1990-2011 - Submitted under the United Nations Framework Convention on Climate Change and  
11 the Kyoto Protocol, Aarhus University, DCE – Danish Centre for Environment and Energy, 1-1202,  
12 2013.

13 Nightingale, P. D., Malin, G., Law, C. S., Watson, A. J., Liss, P. S., Liddicoat, M. I., Boutin, J., and  
14 Upstill-Goddard, R. C.: In situ evaluation of air-sea gas exchange parameterizations using novel  
15 conservative and volatile tracers, *Global Biogeochem. Cy.*, 14, 373-387, 2000.

16 Norman, M., Rutgersson, A., and Sahlée, E.: Impact of improved air-sea gas transfer velocity on  
17 fluxes and water chemistry in a Baltic Sea model, *J. Marine Syst.*, 111, 175-188, 2013.

18 Omstedt, A., Gustafsson, E., and Wesslander, K.: Modelling the uptake and release of carbon  
19 dioxide in the Baltic Sea surface water, *Cont. Shelf. Res.*, 29, 870-885, 2009.

20 Parmentier, F. J. W., Christensen, T. R., Sørensen, L. L., Rysgaard, S., McGuire, A. D., Miller, P.  
21 A., and Walker, D. A.: The impact of lower sea-ice extent on Arctic greenhouse-gas exchange, *Nat.*  
22 *Clim. Change*, 3, 195-202, 2013.

23 Peters, W., Jacobson, A. R., Sweeney, C., Andrews, A. E., Conway, T. J., Masarie, K., Miller, J. B.,  
24 Bruhwiler, L. M. P., Pétron, G., Hirsch, A. I., Worthy, D. E. J., van der Werf, G. R., Randerson, J.  
25 T., Wennberg, P. O., Krol, M. C., and Tans, P. P.: An atmospheric perspective on North American  
26 carbon dioxide exchange: CarbonTracker, *P. Natl. Acad. Sci. USA*, 104, 18925-18930, 2007.

- 1 Plejdrup, M. S. and Gyldenkærne, S.: Spatial distribution of emissions to air - the SPREAD model,  
2 National Environmental Research Institute, Aarhus University, Denmark., 2011.
- 3 Pregger, T., Scholz, Y., and Friedrich, R.: Documentation of the Anthropogenic GHG Emission  
4 Data for Europe Provided in the Frame of CarboEurope GHG and CarboEurope IP, University of  
5 Stuttgart, IER - Institute of Energy Economics and the Rational Use of Energy, 2007.
- 6 Rutgersson, A., Norman, M., and Åström, G.: Atmospheric CO<sub>2</sub> variation over the Baltic Sea and  
7 the impact on air-sea exchange, *Boreal Environ. Res.*, 14, 238-249, 2009.
- 8 Rutgersson, A., Norman, M., Schneider, B., Pettersson, H., and Sahlée, E.: The annual cycle of  
9 carbon dioxide and parameters influencing the air-sea carbon exchange in the Baltic Proper, *J.*  
10 *Marine Syst.*, 74, 381-394, 2008.
- 11 Sarrat, C., Noilhan, J., Lacarrère, P., Masson, V., Ceschia, E., Ciais, P., Dolman, A., Elbers, J.,  
12 Gerbig, C., and Jarosz, N.: CO<sub>2</sub> budgeting at the regional scale using a Lagrangian experimental  
13 strategy and meso-scale modeling, *Biogeosciences*, 6, 113-127, 2009.
- 14 Schneider, B., Kaitala, S., and Maunula, P.: Identification and quantification of plankton bloom  
15 events in the Baltic Sea by continuous *p*CO<sub>2</sub> and chlorophyll a measurements on a cargo ship, *J.*  
16 *Marine Syst.*, 59, 238-248, 2006.
- 17 Schneider, B. and Sadkowiak, B.: Underway *p*CO<sub>2</sub> Measurements in Surface Waters during the  
18 VOS and Research Vruises in the Baltic Sea, Carbon Dioxide Information Analysis Center, Oak  
19 Ridge National Laboratory, U. S. Department of Energy, Oak Ridge, Tenn. , U. S. A., 2012.
- 20 Shark Data Base, SMHI, 2013, <http://www.smhi.se/klimatdata/oceanografi/Havsmiljodata>, last  
21 acces: 1 May 2014.
- 22 Smallman, T. L., Williams, M., and Moncrieff, J. B.: Can seasonal and interannual variation in  
23 landscape CO<sub>2</sub> fluxes be detected by atmospheric observations of CO<sub>2</sub> concentrations made at a tall  
24 tower?, *Biogeosciences*, 11, 735-747, 2014.

1 Sweeney, C., Gloor, E., Jacobson, A. R., Key, R. M., McKinley, G., Sarmiento, J. L., and  
2 Wanninkhof, R.: Constraining global air-sea gas exchange for CO<sub>2</sub> with recent bomb C-14  
3 measurements, *Glob. Biogeochem. Cy.*, 21, GB2015, doi:10.1029/2006GB002784, 2007.

4 Sørensen, L. L., Jensen, B., Glud, R. N., McGinnis, D. F., Sejr, M. K., Sievers, J., Søgaard, D. H.,  
5 Tison, J.-L., and Rysgaard, S.: Parameterization of atmosphere-surface exchange of CO<sub>2</sub> over sea  
6 ice, *The Cryosphere*, 853-866, 2014.

7 Takahashi, T., Sutherland, S. C., Wanninkhof, R., Sweeney, C., Feely, R. A., Chipman, D. W.,  
8 Hales, B., Friederich, G., Chavez, F., Sabine, C., Watson, A., Bakker, D. C. E., Schuster, U., Metzl,  
9 N., Yoshikawa-Inoue, H., Ishii, M., Midorikawa, T., Nojiri, Y., Körtzinger, A., Steinhoff, T.,  
10 Hoppema, M., Olafsson, J., Arnarson, T. S., Tilbrook, B., Johannessen, T., Olsen, A., Bellerby, R.,  
11 Wong, C. S., Delille, B., Bates, N. R., and de Baar, H. J. W.: Climatological mean and decadal  
12 change in surface ocean *p*CO<sub>2</sub>, and net sea-air CO<sub>2</sub> flux over the global oceans, *Deep-Sea Res. PT.*  
13 *II*, 56, 554-577, 2009.

14 Thomas, H., Bozec, Y., de Baar, H. J. W., Elkalay, K., Frankignoulle, M., Schiettecatte, L. S.,  
15 Kattner, G., and Borges, A. V.: The carbon budget of the North Sea, *Biogeosciences*, 2, 87-96,  
16 2005.

17 Thomas, H., Bozec, Y., Elkalay, K., and de Baar, H. J. W.: Enhanced open ocean storage of CO<sub>2</sub>  
18 from shelf sea pumping, *Science*, 304, 1005-1008, 2004.

19 Thomas, H. and Schneider, B.: The seasonal cycle of carbon dioxide in Baltic Sea surface waters, *J.*  
20 *Marine Syst.*, 22, 53-67, 1999.

21 UBA, Air Monitoring Network of the Federal Environment Agency (UBA), Germany Monitoring  
22 site Westerland.

23 United Nations Chapter XXI Law of the Sea, 1984,  
24 [https://treaties.un.org/Pages/ViewDetailsIII.aspx?&src=TREATY&mtdsg\\_no=XXI~6&chapter=21](https://treaties.un.org/Pages/ViewDetailsIII.aspx?&src=TREATY&mtdsg_no=XXI~6&chapter=21&Temp=mtdsg3&lang=en)  
25 [&Temp=mtdsg3&lang=en](https://treaties.un.org/Pages/ViewDetailsIII.aspx?&src=TREATY&mtdsg_no=XXI~6&chapter=21&Temp=mtdsg3&lang=en).

26 Vainio, J., Eriksson, P., Schmelzer, N., Holfort, J., Grafström, T., Lindberg, A. E. B., Lind, L.,  
27 Öberg, J., Viksna, A., Križickis, E., Stanisławczyk I., and Sztobryn, M, 2011, The Ice Season



- 1 2010-11, HELCOM Baltic Sea Environment Fact Sheets, [http://www.helcom.fi/baltic-sea-](http://www.helcom.fi/baltic-sea-trends/environment-fact-sheets/)  
2 [trends/environment-fact-sheets/](http://www.helcom.fi/baltic-sea-trends/environment-fact-sheets/), last access: 23 March 2015
- 3 van der Laan, S., Neubert, R. E. M., and Meijer, H. A. J.: A single gas chromatograph for accurate  
4 atmospheric mixing ratio measurements of CO<sub>2</sub>, CH<sub>4</sub>, N<sub>2</sub>O, SF<sub>6</sub> and CO, *Atmos. Meas. Tech.*, 2,  
5 549-559, 2009.
- 6 van der Laan-Luijkx, I., Neubert, R. E. M., van der Laan, S., and Meijer, H. A. J.: Continuous  
7 measurements of atmospheric oxygen and carbon dioxide on a North Sea gas platform, *Atmos.*  
8 *Meas. Tech.*, 3, 113-125, 2010.
- 9 van der Werf, G. R., Randerson, J. T., Giglio, L., Collatz, G. J., Kasibhatla, P. S., and Arellano, A.  
10 F.: Interannual variability in global biomass burning emissions from 1997 to 2004, *Atmos. Chem.*  
11 *Phys.*, 6, 3423-3441, 2006.
- 12 Wanninkhof, R.: Relationship Between Wind-Speed and Gas-Exchange Over the Ocean, *J. of*  
13 *Geophys. Res-Oceans*, 97, 7373-7382, 1992.
- 14 Weiss, A., Kuss, J., Peters, G., and Schneider, B.: Evaluating transfer velocity-wind speed  
15 relationship using a long-term series of direct eddy correlation CO<sub>2</sub> flux measurements, *J. Marine*  
16 *Syst.*, 66, 130-139, 2007.
- 17 Weiss, R. F.: Carbon Dioxide in Water and Seawater: The Solubility of a Non-ideal Gas, *Mar.*  
18 *Chem.*, 2, 203-215, 1974.
- 19 Wesslander, K., Hall, P., Hjalmarsson, S., Lefevre, D., Omstedt, A., Rutgersson, A., Sahlée, E., and  
20 Tengberg, A.: Observed carbon dioxide and oxygen dynamics in a Baltic Sea coastal region, *J.*  
21 *Marine Syst.*, 86, 1-9, 2011.
- 22 Wesslander, K., Omstedt, A., and Schneider, B.: Inter-annual and seasonal variations in the air-sea  
23 CO<sub>2</sub> balance in the central Baltic Sea and the Kattegat, *Cont. Shelf. Res.*, 30, 1511-1521, 2010.

1 Table 1. Monthly mean fluxes for the period 2005-2010 in the VAT simulation depicting seasonal variation of the air-sea CO<sub>2</sub> exchange. Unit is in Gg C per  
 2 sub-basin. Positive sign indicates release of CO<sub>2</sub> from the ocean to the atmosphere, negative sign indicates uptake of atmospheric CO<sub>2</sub> by the ocean. This sign  
 3 convention is used throughout the paper.

	<i>jan</i>	<i>feb</i>	<i>mar</i>	<i>apr</i>	<i>may</i>	<i>jun</i>	<i>jul</i>	<i>aug</i>	<i>sep</i>	<i>oct</i>	<i>nov</i>	<i>dec</i>	<i>ann</i>
Kattegat	29	-21	-98	-42	-25	-28	-26	-33	-33	-15	14	43	<b>-235</b>
Western Baltic	125	31	-113	-226	-206	-142	-153	-92	60	137	236	140	<b>-203</b>
Central Baltic	804	365	92	-654	-808	-718	-844	-784	-178	481	995	993	<b>-254</b>
Gulf of Finland	49	60	8	-61	-92	-68	-74	-67	1	78	151	117	<b>102</b>
Bothnian Sea	207	120	83	-253	-383	-325	-355	-284	-22	439	529	412	<b>167</b>
Bay of Bothnia	31	23	10	-7	-50	-91	-118	-18	48	205	94	9	<b>137</b>

4  
5

1 Table 2. Annual Danish CO<sub>2</sub> emissions as reported to UNFCCC. The middle row contains the  
 2 annual uptake of CO<sub>2</sub> in the marine area defined as the Danish Exclusive Economic Zone as  
 3 estimated in this study. The bottom rows give this uptake as a percentage of the Danish  
 4 anthropogenic CO<sub>2</sub> emissions.

	2005	2006	2007	2008	2009	2010	6 yr. avg.
CO <sub>2</sub> (Tg C)	14.3	16.5	15.2	14.3	13.6	13.7	<b>14.6</b>
Total Uptake -EEZ (Tg C)	-2.6	-2.4	-2.8	-2.6	-2.6	-2.7	<b>-2.6</b>
% of CO <sub>2</sub>	18	14	18	18	19	20	<b>18</b>

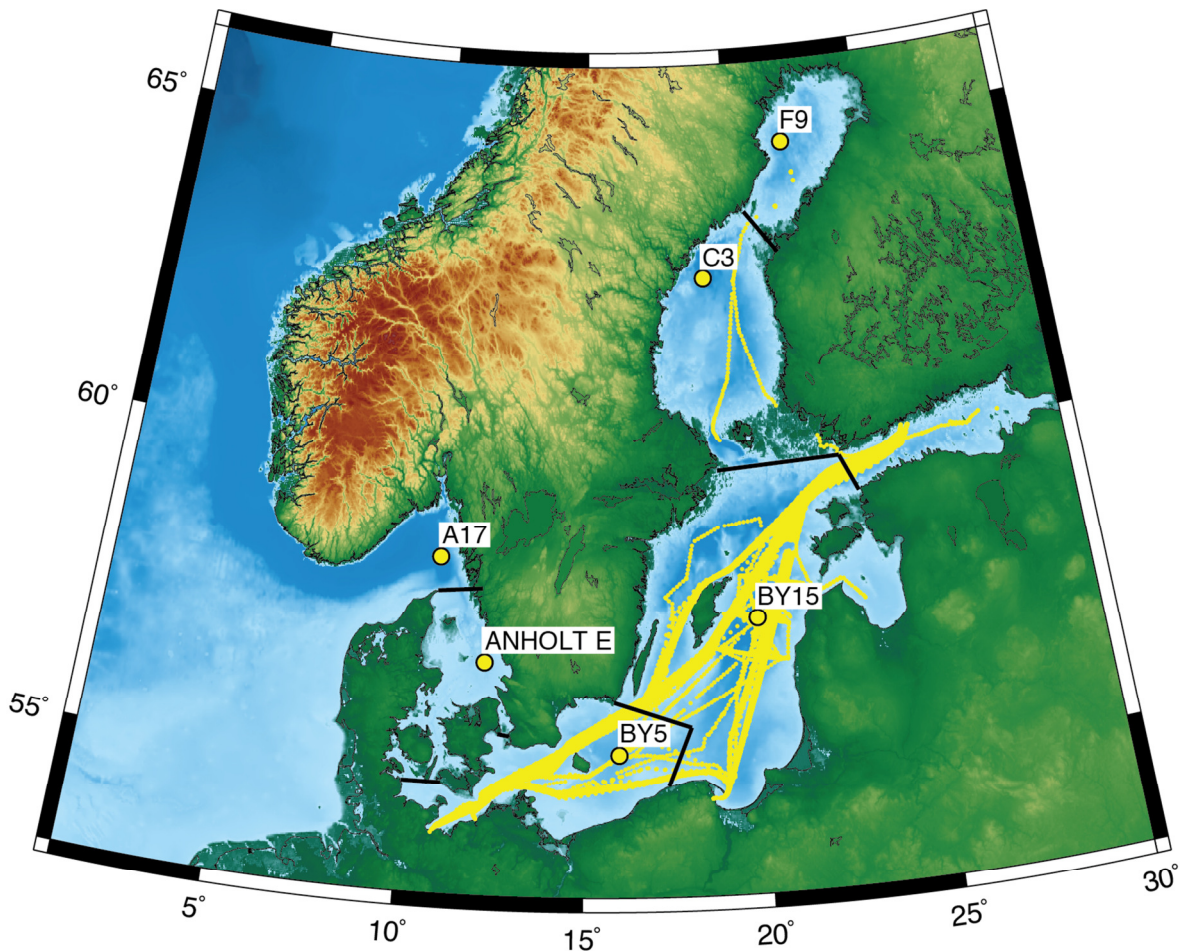
5

6

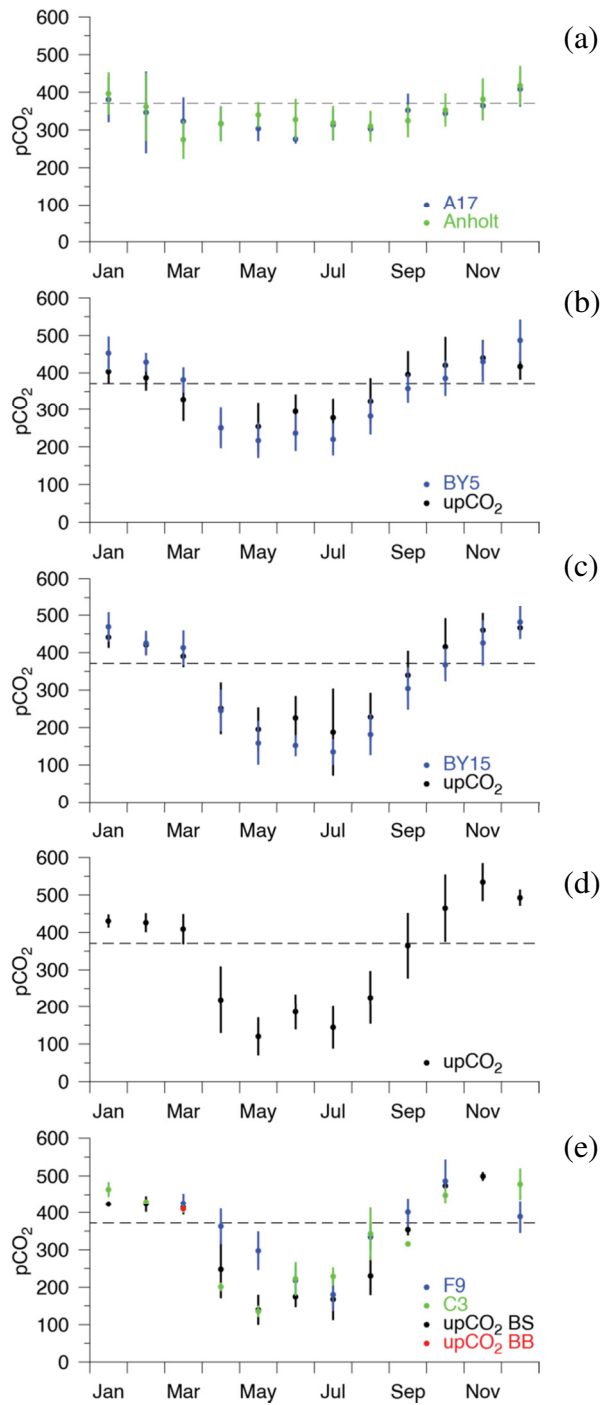
1 Table 3. Present study compared to previous results within the different sub-domains. Study type  
2 indicates the type of previous study (Mod. – model based, MBA – mass balance approach, Meas. –  
3 measurement based, Cru. – cruise based) and its spatial extend (s-b – sub-basins, s-s – site specific).  
4 All shown results are in  $\text{g C m}^2 \text{ yr}^{-1}$ .

	<i>Previous results</i>	<i>Study</i>	<i>Study type</i>	<i>Present Study</i>
Kattegat	-40.0	Gustafsson et al. (2014)	Mod., s-b	-7.0
	19.0	Norman et al. (2013)	Mod., s-b	
	-13.9	Wesslander et al. (2010)	Meas., s-s	
Western Baltic	-34	Gustafsson et al. (2014)	Mod., s-b	-3.1
	-36.0	Kuss et al. (2006)	Meas., s-s	
	-14.4 to 17.9	Norman et al. (2013)	Mod., s-b	
	28.1	Wesslander et al. (2010)	Meas., s-s	
Baltic Proper	-4.2 to -4.3	Norman et al. (2013)	Mod., s-b	-1.5
	-10.8	Schneider and Thomas(1999)	Cru., s-b	
	19.7	Wesslander et al. (2010)	Meas., s-s	
Bothnian Sea	2.2	Gustafsson et al. (2014)	Mod., s-b	2.2
	-8.8	Löffler et al. (2012)	Cru., s-b	
	-0.6	Norman et al. (2013)	Mod., s-b	
Bay of Bothnia	12.0	Gustafsson et al. (2014)	Mod., s-b	3.8
	1.7	Löffler et al. (2012)	Cru., s-b	
	4.3	Norman et al. (2013)	Mod., s-b	
Gulf of Finland	7.4	Norman et al. (2013)	Mod., s-b	4.3
Total Baltic Sea	2.7	Kulinski and Pempkowiak (2010)	MBA, s-b	-0.7
	-4.3	Gustafsson et al. (2014)	Mod., s-b	
	-2.6	Norman et al. (2013)	Mod., s-b	

5  
6

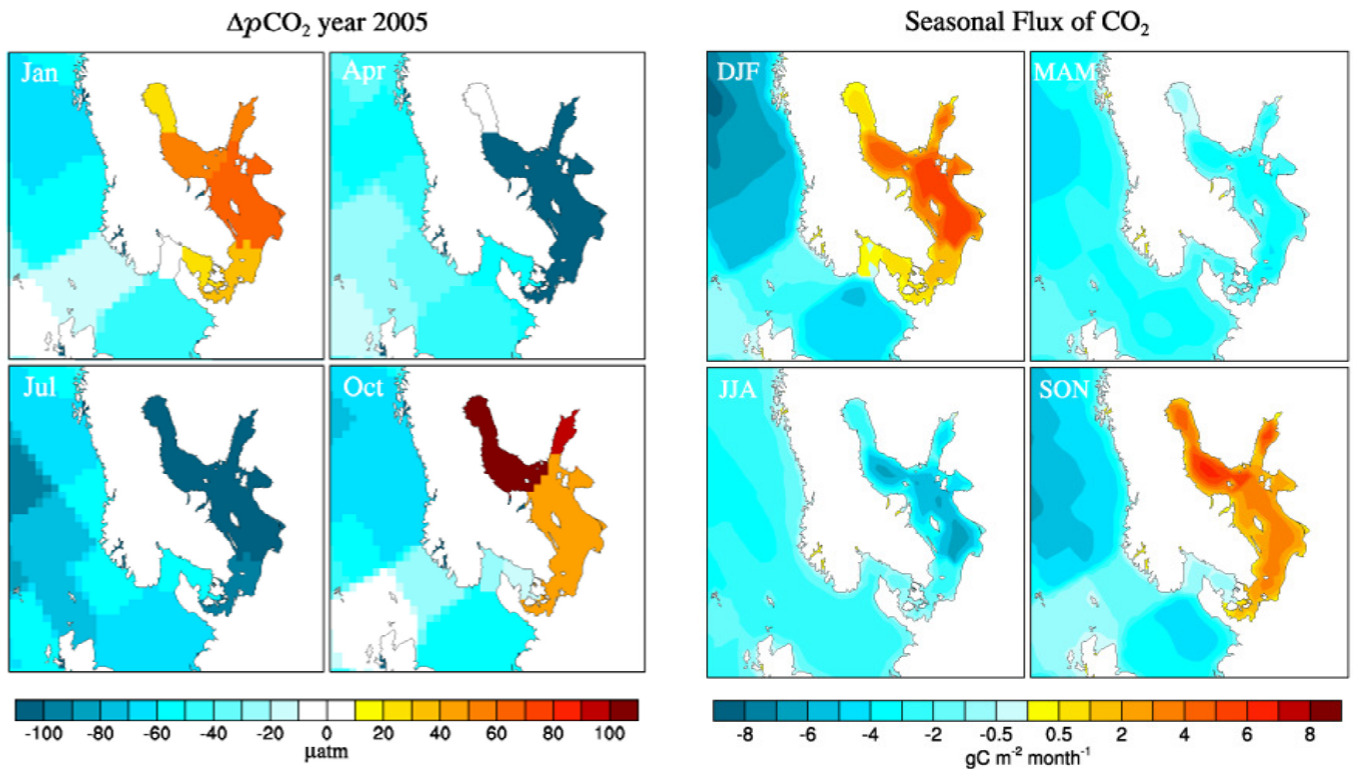


1  
 2 Figure 1. The locations of the six monitoring stations in the Baltic Sea, where surface  $p\text{CO}_2$  values  
 3 are calculated (Shark Data Base, 2013). The stations are located in Skagerrak (A17), Kattegat and  
 4 the Danish straits (Anholt E), the Western Baltic Sea (BY5), Baltic proper (BY15), the Bothian Sea  
 5 (C3) and the Bay of Bothnia (F9). Data from underway measurements of surface  $p\text{CO}_2$  are shown  
 6 with yellow and covers in particular the area between Kiel and Helsinki. The division of the six sub-  
 7 domains is indicated with black lines.  
 8



1 Figure 2. Monthly averaged surface  $p\text{CO}_2$  values from the six monitoring stations and from  
 2 underway  $p\text{CO}_2$  data in the sub-domains in the study region. Monthly averaged values are shown  
 3 with bullets together with the standard deviations. a) Values from monitoring stations in Skagerrak  
 4 (A17, blue) and Kattegat (Anholt E, green), b) station BY5 (blue) and underway  $p\text{CO}_2$  in the  
 5 Western Baltic Sea (black), c) station BY15 (blue) and underway  $p\text{CO}_2$  from the Baltic Proper  
 6 (black), d) underway  $p\text{CO}_2$  data from the Gulf of Finland and e) station F9 (blue), C3 (green) and

- 1 underway  $p\text{CO}_2$  data from the Bothnian Sea (black) and underway  $p\text{CO}_2$  from March in the Bay of
- 2 Bothnia (red).
- 3



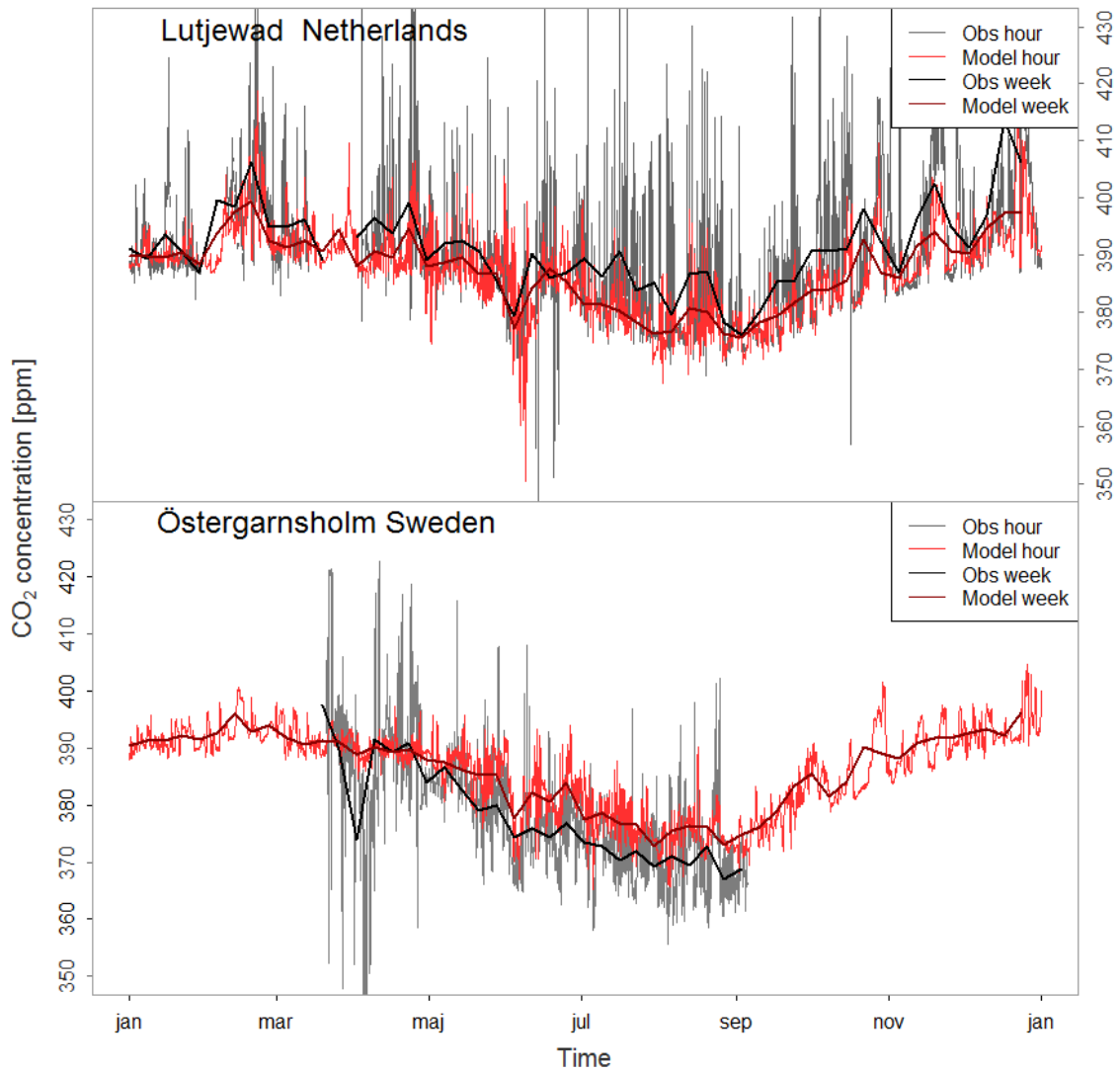
1  
2  
3  
4  
5  
6  
7  
8  
9  
10  
11  
12  
13  
14

(a)

(b)

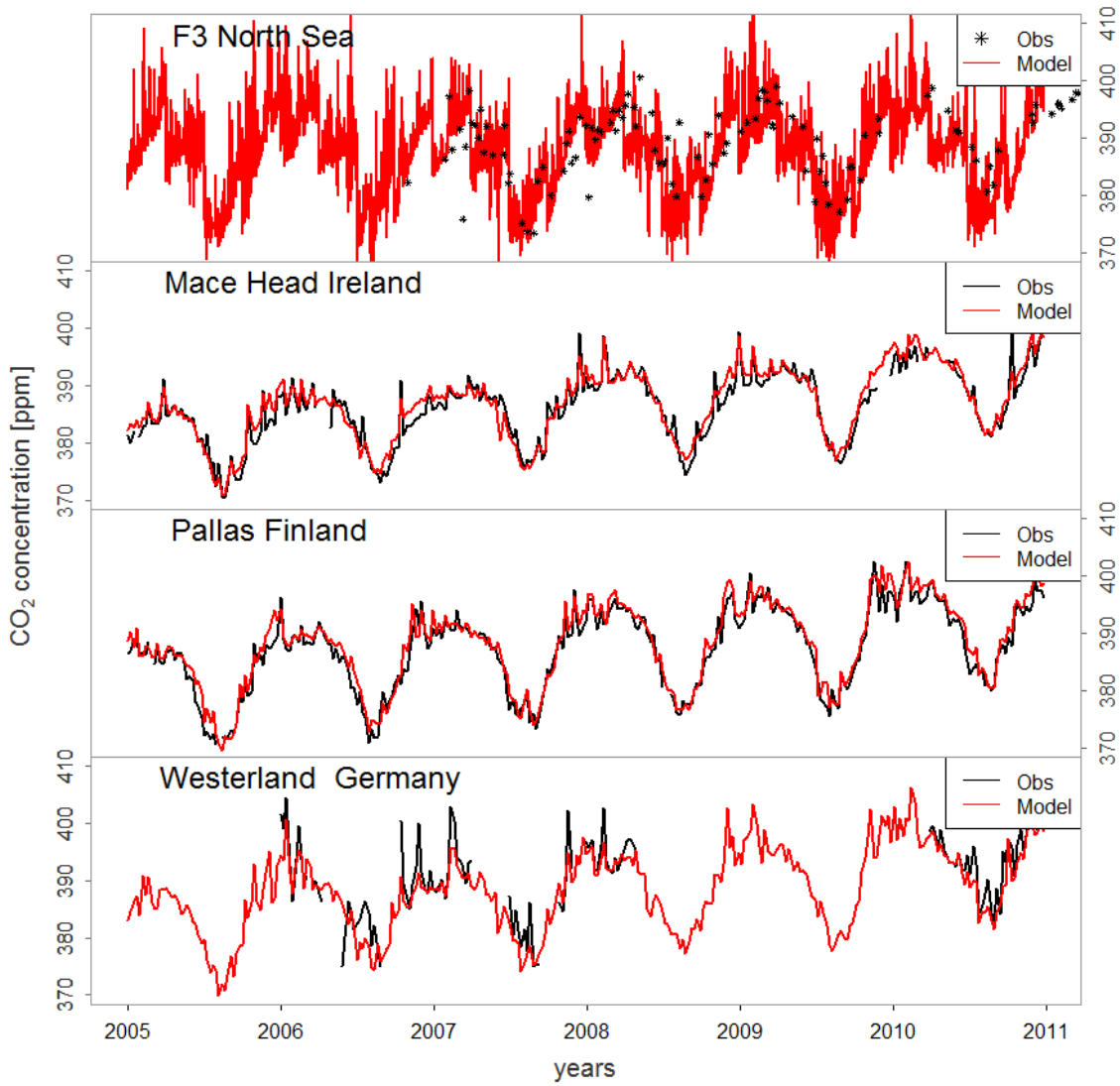
Figure 3. a)  $\Delta p\text{CO}_2$  for selected months during 2005. For the calculations of  $\Delta p\text{CO}_2$  the combined surface map of the global  $p\text{CO}_2$  climatology by Takahashi et al. (2009) and the climatology for the Baltic Sea constructed in this study is used. The coarse resolution of the global climatology is clearly visible along the west coast of Norway. Periods of under and over-saturation are seen which indicates the direction of the air-sea CO<sub>2</sub> flux (positive  $\Delta p\text{CO}_2$  indicates release of CO<sub>2</sub> to atmosphere, negative values indicate uptake of atmospheric CO<sub>2</sub>). b) The mean seasonal air-sea CO<sub>2</sub> flux for the years 2005 to 2010 in  $\text{g C m}^{-2} \text{month}^{-1}$  for the VAT simulation. Positive sign indicates release of CO<sub>2</sub> from the ocean to the atmosphere, negative sign indicates uptake of atmospheric CO<sub>2</sub> by the ocean. This sign convention is used throughout the paper.





1  
 2 Figure 4. One hour averages of modelled and continuously measured atmospheric CO<sub>2</sub>  
 3 concentrations in 2007. Also weekly averages of both modelled and measured CO<sub>2</sub> concentrations  
 4 are shown.

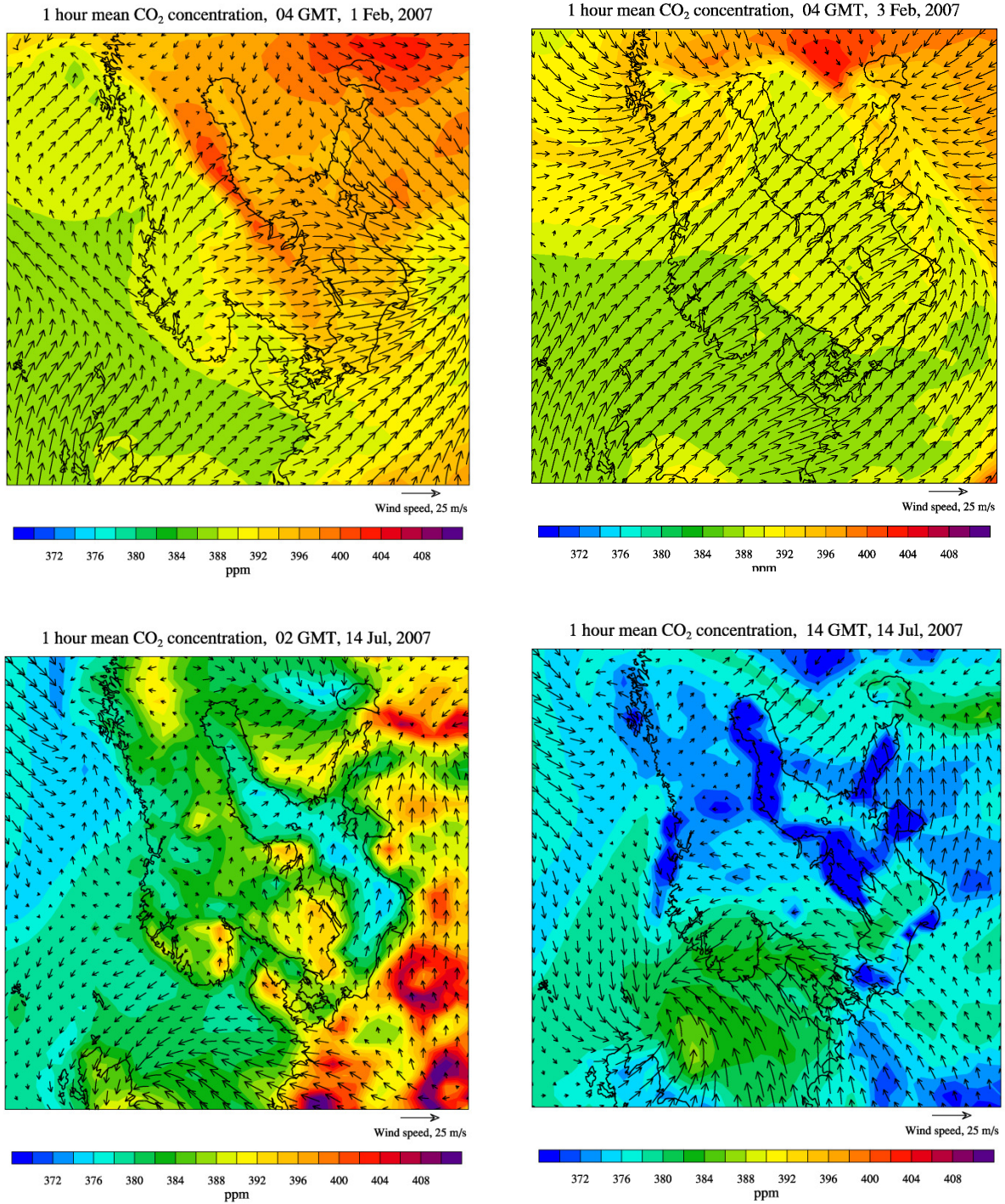
5



1  
 2 Figure 5. Top panel shows hourly averages of modelled atmospheric CO<sub>2</sub> concentrations compared  
 3 to flask measurement at F3. The three panels below include comparisons of weekly averages of  
 4 modelled and continuous measurements of CO<sub>2</sub> at MHD, PAL and WES for the period 2005-2010.

5  
 6  
 7  
 8  
 9

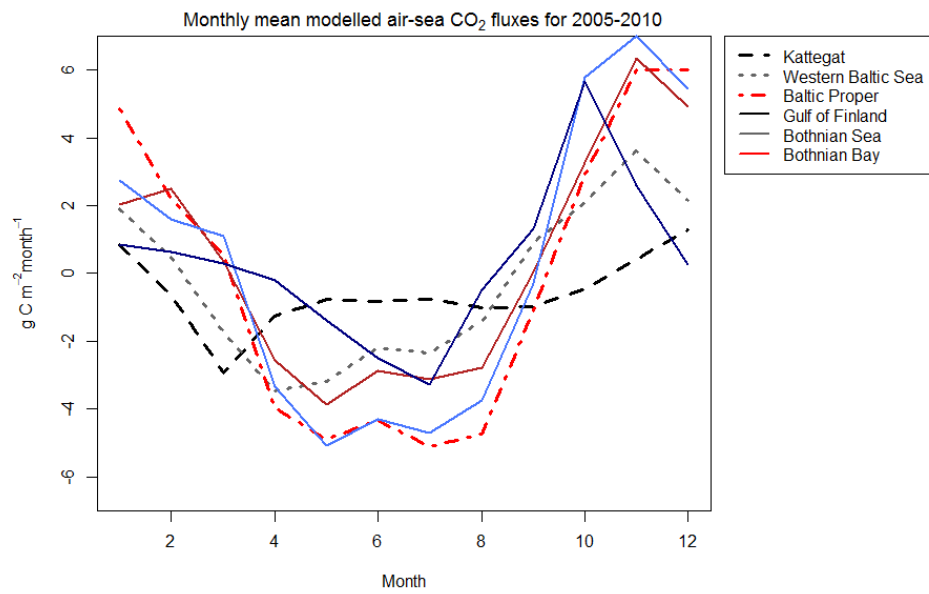
1



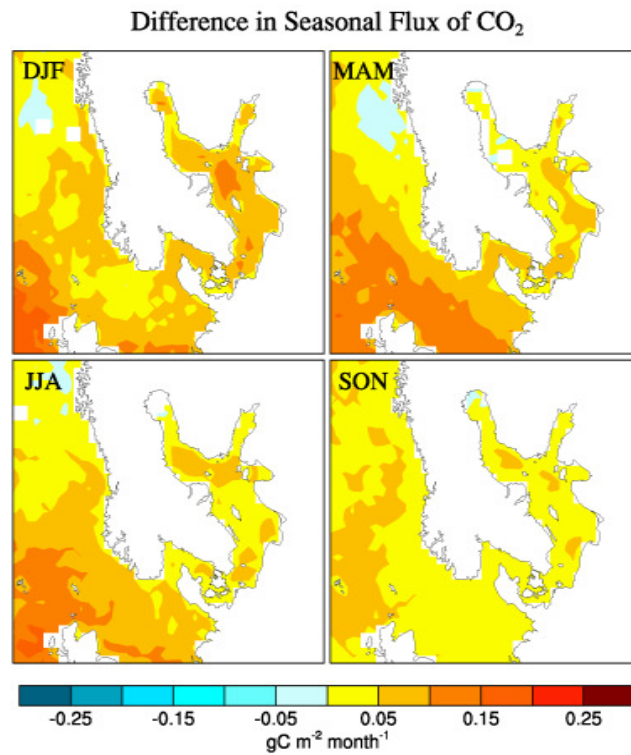
2

3 Figure 6. Examples of the simulated variability of atmospheric CO<sub>2</sub> in the study area shown here as  
4 extracted from the European domain in DEHM with a 50 km x 50 km resolution. Top panel: Two

1 situations for February 2007. Continental air masses cover the Baltic region on 1 February, while  
2 marine air masses are dominating on 3 February. Bottom panel: The diurnal variability on 14 July  
3 2007 (night time (left) and day time (right)).



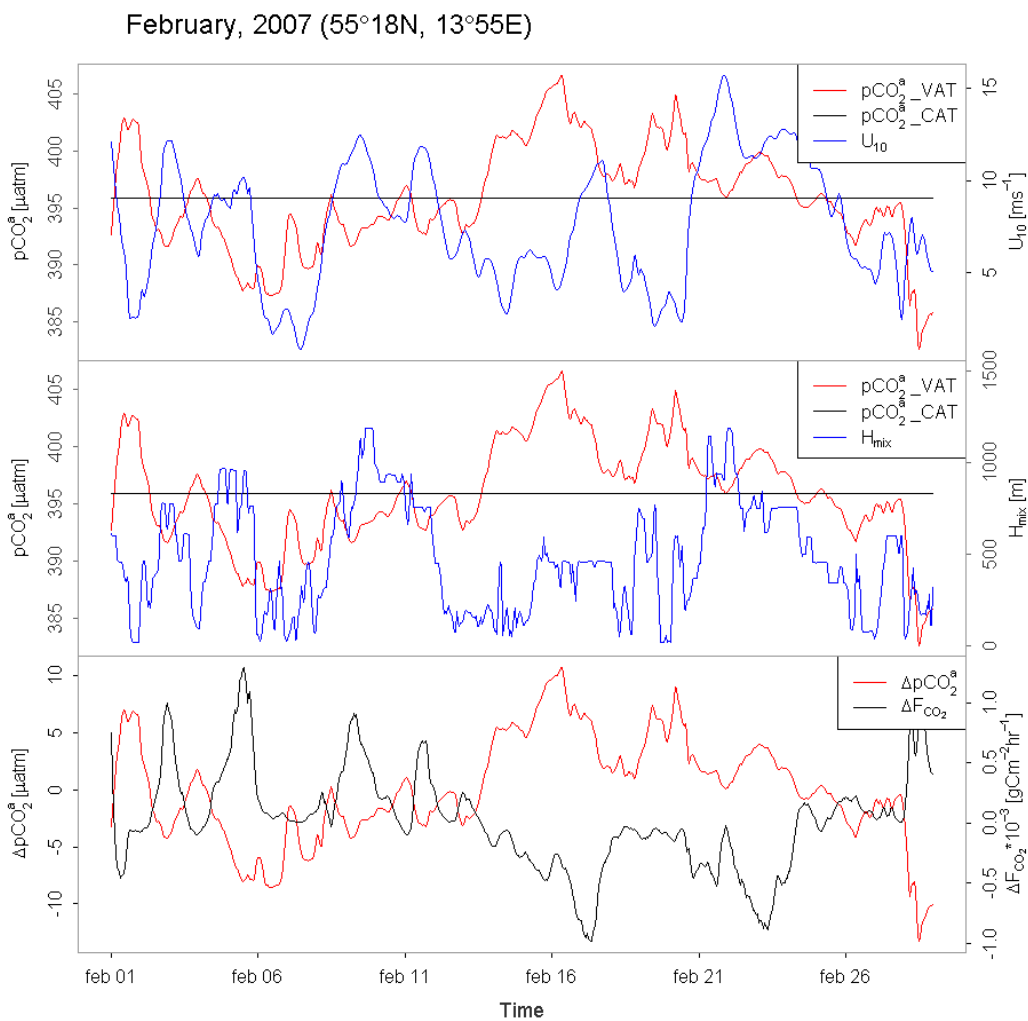
1  
 2 Figure 7. The monthly mean air-sea CO<sub>2</sub> flux for the years 2005 to 2010 in the six sub-basins in g C  
 3 m<sup>2</sup> pr. month for the VAT simulation.  
 4



1

2 Figure 8. The seasonal flux difference between the VAT and CAT simulations for the period 2005  
 3 to 2010 in g C m<sup>-2</sup> pr. month calculated as VAT-CAT. In winter both the fluxes in VAT and CAT  
 4 are positive, but VAT is larger than CAT, and thus the difference is positive. In summer both the  
 5 fluxes in VAT and CAT are negative, but CAT is numerical larger than VAT, and thus the  
 6 difference is also positive.

7



1

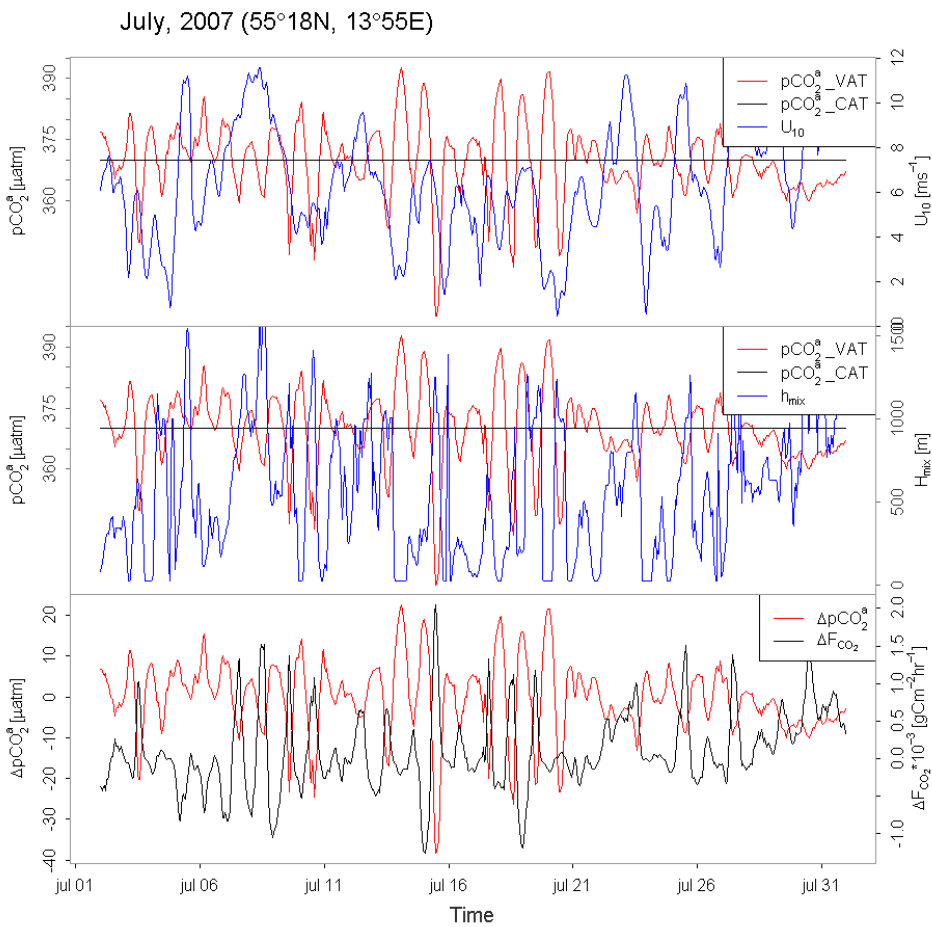
2 Figure 9. Time series of driving parameters as extracted from the simulations at the site south of

3 Sweden (55°18' N, 13°55' E) February 2007. Top panel:  $p\text{CO}_2^a$  for VAT and CAT together with  $u_{10}$ .

4 Middle panel:  $p\text{CO}_2^a$  for VAT and CAT together with  $h_{\text{mix}}$ . Bottom panel: Difference in  $p\text{CO}_2^a$

5 ( $\Delta p\text{CO}_2^a$ ) and  $F_{\text{CO}_2}$  ( $\Delta F_{\text{CO}_2}$ ) between VAT and CAT.

6

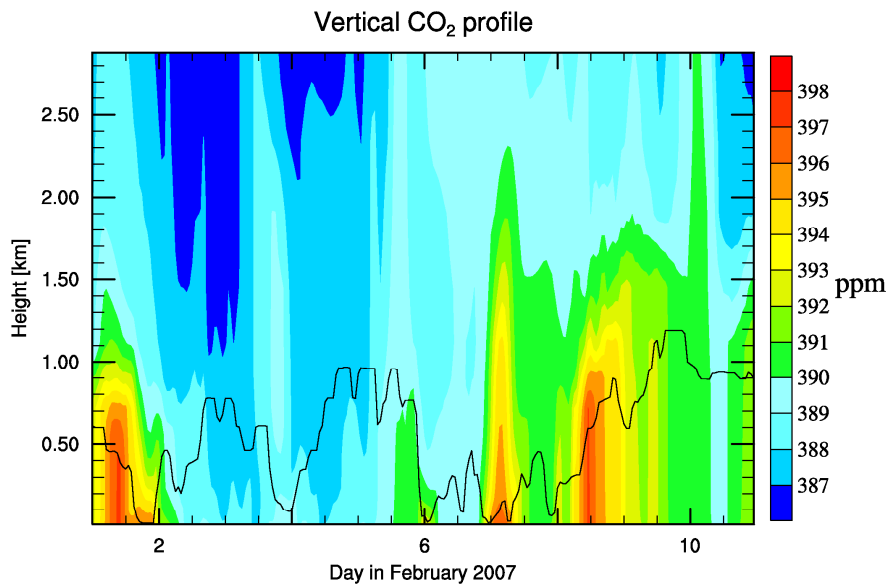


1

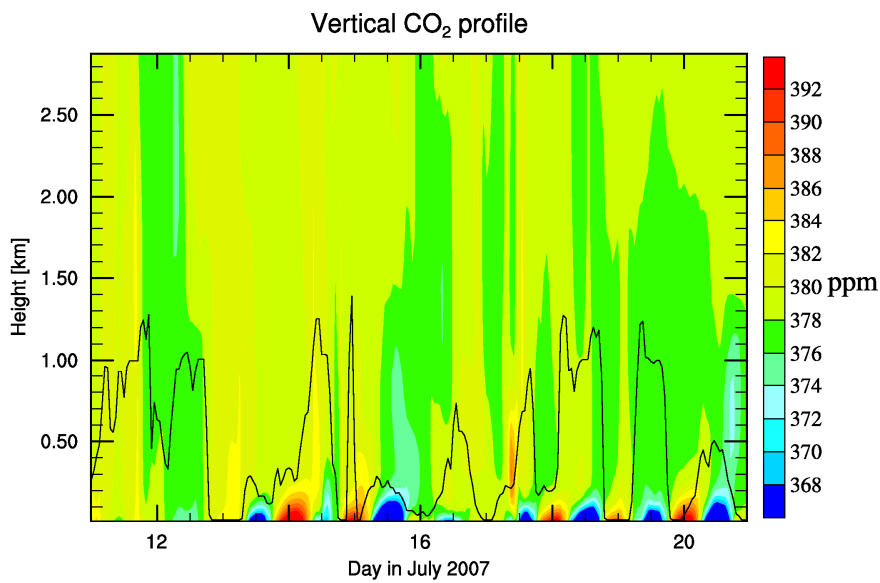
2 Figure 10. Simulated parameters as in Fig. 9 at the site south of Sweden (55°18' N, 13°55' E), but for  
 3 July, 2007. Top panel:  $p\text{CO}_2^a$  for VAT and CAT together with  $u_{10}$ . Middle panel:  $p\text{CO}_2^a$  for VAT and  
 4 CAT together with  $h_{\text{mix}}$ . Bottom panel: Difference in  $p\text{CO}_2^a$  ( $\Delta p\text{CO}_2^a$ ) and  $F_{\text{CO}_2}$  ( $\Delta F_{\text{CO}_2}$ ) between  
 5 VAT and CAT.

6





1



2

3 Figure 11. Simulated vertical profiles of atmospheric CO<sub>2</sub> at the site south of Sweden (55°18N,  
 4 13°55E) in units of ppm. Top panel: 1-10 February 2007. Bottom panel: 11 – 20 July 2007. The  
 5 black line represents the mixing height in km. Note the different scales used in the two plots.

6